

Motion Planning in the Presence of Directional and Regional Avoidance Constraints Using Nonlinear, Anisotropic, Harmonic Potential Fields: A Physical Metaphor

Samer A. Masoud and Ahmad A. Masoud

Abstract—Motion planning, or goal-oriented, context-sensitive, intelligent control is essential if an agent is to act in a useful manner. This paper suggests a new class of motion planners that can mark a constrained trajectory to a target zone in an environment that need not necessarily be *a priori* known. The novelty of the suggested planner lies in its ability to enforce region avoidance and direction satisfaction constraints jointly. To the best of the authors' knowledge, this is the first time that directional constraints have been addressed in the motion planning literature. To build such a planner, the potential field approach is used for inducing the control action. In addition, to cope with the presence of the above constraints (in particular, the directional constraints), a new type of potential field, called the nonlinear anisotropic harmonic potential field, is suggested. The planner has applications in traffic management and operations research among others. Development of the approach, proofs of correctness, and simulation results are supplied.

Index Terms—Harmonic potential fields, intelligent control, mobile robot, motion planning, navigation.

I. NOMENCLATURE

IMC	Intelligent motion controller.
HLC	High-level controller.
LLC	Low-level controller.
NC	Navigation control.
BVP	Boundary value problem.
PDE	Partial differential equation.
ODE	Ordinary differential equation.
HPC	Hybrid PDE-ODE controller.
EHPC	Evolutionary HPC.
LFC	Lyapunov function candidate.
LF	Lyapunov function.
AI	Artificial intelligence.
AL	Artificial life.
P-Type	Pheno type of behavior.
G-Type	Geno type of behavior.

FAC	First attempt completeness.
PF	Potential field.
HPF	Harmonic potential field.
NAHPF	Nonlinear anisotropic HPF.
PRF	Purpose field component of the multiagent control.
CRF	Conflict resolving field component of the multiagent control.
X	N -dimensional state vector.
X_T	Target state.
u	M -Dimensional control vector.
∇	Gradient operator.
∇^2	Laplacian operator.
$\nabla \cdot$	Divergence operator.
O	Avoidance region.
O'	Expanded avoidance region ($O \subset O'$).
Γ	Boundary of O ($\Gamma = \partial O$).
n	Unit vector normal to Γ .
Ω	Workspace ($\Omega = R^N - O$).
Ω'	Directionally constrained subset of Ω ($\Omega' \subset \Omega$).
Γ'	Boundary of Ω' ($\Gamma' = \partial \Omega'$).
Γ'_b	Subset of Γ' on which unstable local equilibrium form.
π	Zero-measure, unstable, local, equilibrium set ($\pi \in \Omega$).
Ψ	Vector function marking preferred direction of motion in Ω' .
S	Sphere representing the sensed region around $X(t)$.
ρ	Radius of S .
Γ_s	Subset of Γ newly sensed by S .
ω_s	Subset of Ω' newly sensed by S .
Γ_c	Accumulating representation of Γ .
Ω_c	Accumulating representation of Ω' .
ϕ	Empty set.
Q	Binary indicator time function that marks the detection of new constraints by S .
t_i	Time at which new constraints are detected.
t'_I	Time at which new control policy is generated ($t_{(i+1)} > t'_I > t_i$).
σ_{xi}	Bimodal admittance of a directional constraint.
σ_b	Backward mode of σ_{xi} .
σ_f	Forward mode of σ_{xi} .
Σ	Bimodal admittance matrix.
Φ	Unit step function.

Manuscript received March 19, 2001; revised September 18, 2002. The development of this work was personally funded by the authors. This work was supported by King Fahd University of Petroleum and Minerals and Jordan University of Science and Technology.

S. A. Masoud is with the Mechanical Engineering Department, Jordan University of Science and Technology, Irbid, Jordan (e-mail: masoud@just.edu.jo).

A. A. Masoud is with the Electrical Engineering Department, King Fahd University of Petroleum and Minerals, Dhahran 31261, Saudia Arabia (e-mail: masoud@kfupm.edu.sa).

Digital Object Identifier 10.1109/TSMCA.2002.807030

δ	Dirac-Delta function.
G	Directed graph.
N	Set of vertices.
Z	Corresponding set of edges.
K	Number of vertices in a graph.
N_I	Initial vertex.
N_T	Target vertex.
T_n	Normalized CPU execution time.
N_g	Null space of g .

II. INTRODUCTION

UTILITY and meaning in the behavior of an agent are highly contingent on the agent's ability to semantically embed its actions in the context of its environment. Such an ability is cloned into an agent using a class of intelligent motion controllers (IMCs) that are called motion planners. Despite the diversity of motion planning methods [1]–[3], all existing techniques, to the best of the authors' knowledge, are unified in considering isotropic workspaces (a workspace is an admissible subset of state space) where, at any point in the workspace, the agent is permitted to arbitrarily direct the motion of its state, motion actuators permitting. Practical workspaces, on the other hand, face a serious traffic management task that is usually handled by dividing the available space into structured domains each assigned a set of rules for directing traffic [4], [5]. In most cases, such rules extend beyond region avoidance to that of restricting the direction along which motion is allowed to proceed (Fig. 1). In a typical environment it is customary to find regions where traffic is prohibited, regions where traffic flow is regulated (e.g., ENTER and EXIT signs, etc.) and others where traffic is free. It is unusual to find a modern road or building where the above does not apply. Tackling such a situation requires that motion to the target be conditioned with joint regional-avoidance directional-satisfaction constraints.

Directional constraints acquire special significance when they are applied to a directed graph (di-graph) [6], [7] in order to govern motion between its vertices. An intelligent controller that is configured to operate in this manner may be used for finding the shortest route in a di-graph. Finding the shortest route on a graph in a manner that is sensitive to direction is an important problem in operations research with numerous applications in equipment replacement, scheduling of complex projects, and least cost travel [8]. Other applications of directional constraints are demonstrated in the sequel.

From an AI point of view, the incorporation of directional constraints along with regional avoidance in governing the actions of an agent while making no assumptions about the geometry or topology of the environment is a formidable planning challenge. To the best of the authors' knowledge, this situation has not yet been addressed in the motion planning literature. It fundamentally differs from planning under nonholonomic constraints [9] in which an agent may not be able to project motion along certain directions in the workspace due to the inability of its actuators to drive motion along these directions (i.e., the constraints in the control space, which limit the efficacy of the motion actuators, are the ones responsible for this behavior). On the other hand, directional constraints that are imposed in the

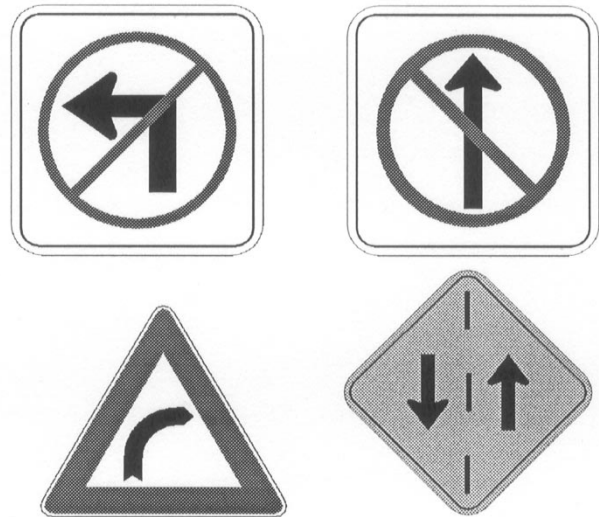


Fig. 1. Signals for directing traffic.

admissible region of state space (i.e., the workspace) cannot be violated even if the agent's actuators have the ability to do so.

While there are many planning approaches from which one may choose a candidate to modify in order to incorporate directional constraints, the authors believe that the PF approach to motion planning, in particular the HPF approach, is an ideal candidate for such a choice. To the best of the authors' knowledge, the PF approach was the first to be used to generate a paradigm for motion guidance [10], [11]. The paradigm began from the simple idea of an attractor field situated on the target and a repeller field fencing the obstacles. Several decades later, the paradigm surfaced again through the little-known work of Loeff and Soni which was carried out in the early 1970s [12], [13]. Not until the mid-1980s did this approach achieve recognition in the path planning literature through the works of Khatib [14], Krogh [15], [16], Takegaki and Arimoto [17], and Nishida *et al.* [18] in Japan, and Pavlov and Voronin [19], Vereshchagin *et al.* [20], Malyshev [21], Aksenov *et al.* [22], as well as Petrov and Sirota [23], [24] in the former Soviet Union. It ought to be mentioned that the work of Petrov and Sirota is probably the first attempt for constructing a provably-correct, sensor-based motion planner that can guide a robot with an arbitrary shape in a cluttered, unknown environment using only highly localized sensory information. In [23], the planner was developed for a two-dimensional (2-D) environment. Later, in [24], the planner was generalized for the three-dimensional (3-D) case. Andrews and Hogan also worked on the idea in the context of force control [25]. Although a paradigm to describe motion using HPFs has been available for more than three decades [26]–[28] it was not until 1987 that Sato [29] formally used it as a tool for motion planning. Unfortunately, the work was written in Japanese and had very little exposure (an English version of the work may be found in [30]). A few years after, the approach was formally introduced to the robotics and intelligent control literature through the independent work of Connolly *et al.* [31], Prassler [32] and Tarassenko *et al.* [33], who demonstrated the approach using an electric network analogy, Lei [34] and Plumer [35], who used a neural network setting, and Keymeulen *et al.* [36], [37] and

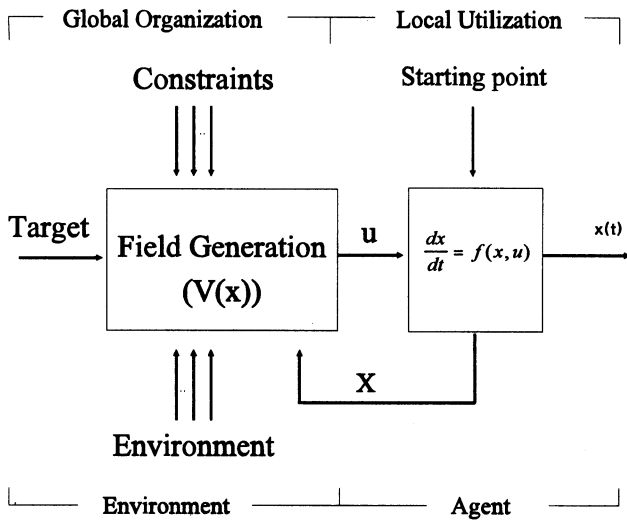


Fig. 2. Hybrid, PDE-ODE control structure.

Akishita *et al.* [38], who utilized a fluid dynamic metaphor in their development of the approach (the neural net suggested by Lei was also motivated by a fluid dynamic metaphor). Cheng *et al.* [39]–[41] utilized harmonic potential fields for the construction of silicon retina, VLSI wire routing, and robot motion planning. A unity resistive grid was used for computing the potential. In [42], Dunskeya and Pyatnitskiy suggested a potential field whose differential properties are governed by the inhomogeneous Poisson equation for constructing a nonlinear controller for a robotic manipulator taking into consideration obstacles and joint limits. Other work may be found in [43]–[68]. While not directly related to robot motion planning, Li *et al.* [69] used the harmonic potential approach in the Dirichlet setting to plan the motion of the pixels of an image so that controlled shape transformation may be achieved.

The harmonic potential field approach is an expression of the, more general, hybrid, partial differential equation-ordinary differential equation (PDE-ODE) paradigm to motion synthesis (Fig. 2) [50], [70]–[73]. A hybrid, PDE-ODE controller (HPC) functions to convert the data that is available to the agent about its environment into information that is encoded in the structure of the differential control action group which the agent uses to steer itself. In this class of controllers the conversion mechanism is constructed in conformity with the AL approach to behavior generation [74]. To achieve this mode of operation, first the lucidity of the control action is established by inducing the control action group on a potential field surface using a vector partial differential operator. The behavior of each member of the group (differential control action) is constrained with respect to the other members in its immediate neighborhood using a proper partial differential operator (G-type of behavior). The group control action (P-type) evolves in space and time as a result of the interpretation of the G-type in the context of the environment. This is achieved by using boundary conditions to factor the influence of the environment in the behavior generation process. Fig. 3 shows an evolving control action group in an HPC. In essence, HPCs function to convert available data about the environment into information the agent uses to steer its actions. To our knowledge, Asimov was the first to describe the

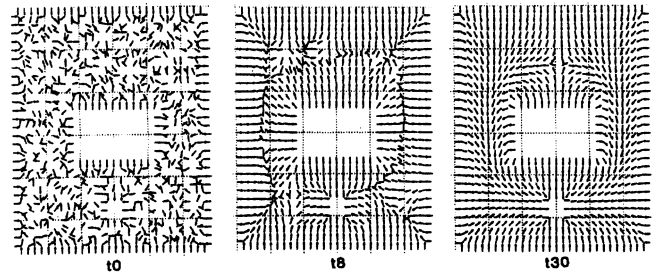


Fig. 3. Evolution of the control field in an HPC.

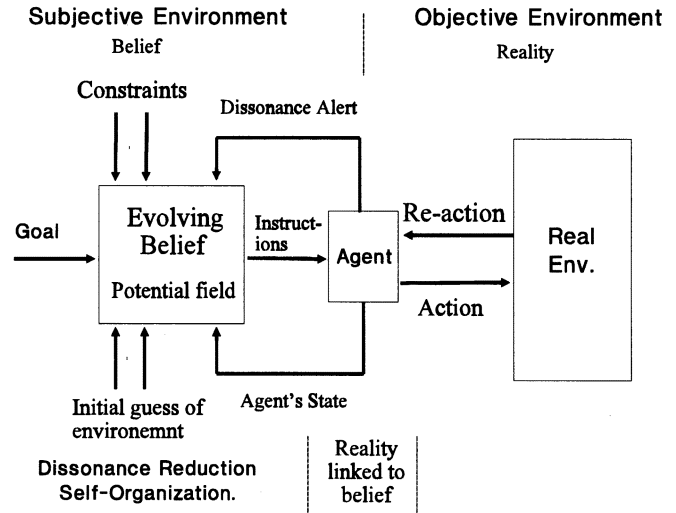


Fig. 4. Evolutionary, hybrid, PDE-ODE control structure constructed by coupling the HPC structure to a hybrid discrete time—continuous time system.

utilization of PFs in the context of an AL paradigm for motion synthesis and behavior generation. In [75], he used allegory to describe how the behavior of a robot unfolds (P-Type) as a result of the interpretation of a set of behavioral rules (G-Type) in the context of the robot’s environment.

Implicit in the ability of an agent to successfully reach its target is the availability of a necessary and sufficient level of data for the HPC to grind into action. Unfortunately, in a realistic situation, no such guarantees are provided. This is a serious weakness of HPCs that negatively impacts on their ability to steer the utilizing agent to its target state. This weakness, however, may be remedied by grounding the agent in its physical environment using evolutionary, hybrid, PDE-ODE controllers (EHPCs) [70]–[72].

An evolutionary, hybrid, PDE-ODE (Fig. 4) controller consists of two parts:

- 1) a discrete time-continuous time system to couple the discrete-in-nature data acquisition process to the continuous-in-nature action release process;
- 2) a hybrid, PDE-ODE controller to convert the acquired data into information that is encoded in the structure of the differential control action group.

EHPCs are situated, embodied, intelligent, and emergent mechanisms for behavior generation [76]. They require no *a priori* knowledge of their multidimensional environment to guarantee that an agent with an arbitrary unknown shape

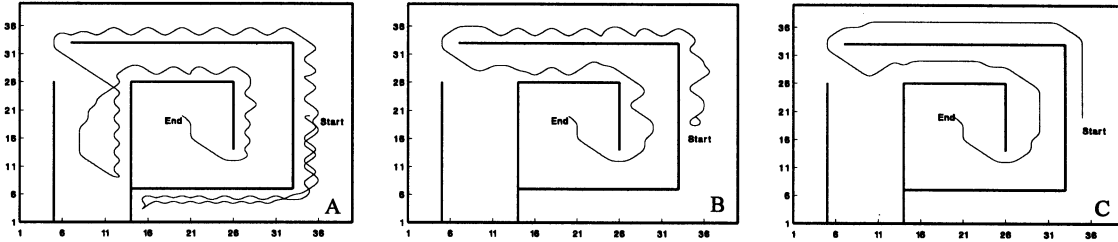


Fig. 5. EHPC navigating an unknown maze. (a) First attempt. (b) Second attempt. (c) Third attempt.

will converge to its target from the first attempt (first attempt completeness (FAC) characterizes the state where initially the agent has no information about its environment). Moreover, in this class of planners, the range of the sensors has no influence on convergence. Even local sensing, such as tactile sensing, is enough to guarantee that the controller can mark a constraint-satisfying trajectory to the target in a multidimensional environment. The range of the sensors controls only the speed at which this trajectory can be carved. Fig. 5 shows three attempts of a point agent to reach its target at the center of a maze. Despite the total lack of *a priori* knowledge about the maze and the use of proximity sensing, the agent manages to reach its target at every attempt, each time enhancing its performance until it converges along an optimal path to the target.

In this paper, the capabilities of EHPCs are upgraded to enable them to plan in nonlinear, anisotropic workspaces supporting joint directional-regional avoidance constraints. This is accomplished by modifying the second component of an EHPC, the hybrid, PDE-ODE controller so that it can incorporate direction among the set of constraints it is enforcing. The core of the modified HPC component is a new group of PFs called NAHPF. This new group of PFs makes it possible to condition the induced control with the desired directional and regional avoidance constraints.

Section II of the paper contains the problem formulation. Section III describes the physical metaphor used in deriving the NAHPF and in turn the modified HPC. Section IV contains the mathematical description of the modified HPC. Section V contains proofs of the validity of the suggested HPC. Results, and conclusions are placed in Section VI and VII, respectively.

III. FORMULATION

In the following, the behaviors of the modified HPC and EHPCs are mathematically described.

A. Problem Formulation, HPC

In its most general form, an HPC is required to synthesize a control signal u for a dynamical system that is described by the nonlinear state-space equation (Fig. 6)

$$\dot{X} = f(X, u)$$

$$\text{such that } \lim_{t \rightarrow \infty} X(t) \rightarrow X_T, \& X(t) \cap O \equiv \phi \quad \forall t \quad (1)$$

where X is an N -dimensional vector describing the agent's state in its natural coordinates, u is an N -dimensional control

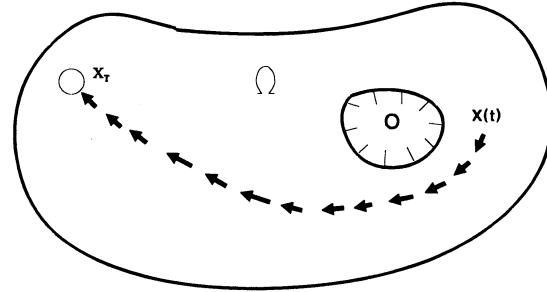


Fig. 6. Domain of an existing HPC.

vector, $f: R^N \times R^M \rightarrow R^N$, X_T is the target state, O is the set of forbidden regions in state space which the agent should always avoid, and Γ is the boundary of O ($\Gamma = \partial O$). While ongoing work is focused on developing HPCs that can realistically tackle both the dynamics and kinematics of an agent [77], here, the focus is only on kinematics, i.e., the equation of motion is

$$\dot{X} = u. \quad (2)$$

In addition, the HPC used here is expressed using an HPF (V) in the Dirichlet setting. Other ways for expressing an HPC may be found in [50] and [73]. For this case, existing HPCs are required to synthesize the control signal

$$u = -\nabla V(X, \Gamma, X_T) \quad (3)$$

so that for a system described by (2), the conditions in (1) are satisfied. V is constructed by solving the BVP

$$\begin{aligned} \nabla^2 V(X) &\equiv 0, & X \in \Omega \\ V(X_T) &= 0, & V(X)|_{X \in \Gamma} = C \end{aligned} \quad (4)$$

where Ω is the workspace ($\Omega = R^N - O$), and ∇^2 , ∇ are the Laplacian and gradient operators, respectively. The directional constraints that the modified HPC is required to enforce are defined on Ω' ($\Omega' \subset \Omega$). They assume the form of the vector field $\Psi(X)$, $X \in \Omega'$, $\Psi: R^N \rightarrow R^N$. The compliance of the agent with these constraints is detected using the inner product

$$\dot{X}^t \Psi(X) \quad (5)$$

such that if $\dot{X}^t \Psi(X) > 0$, the constraints are enforced, and if $\dot{X}^t \Psi(X) \leq 0$, the constraints are violated.

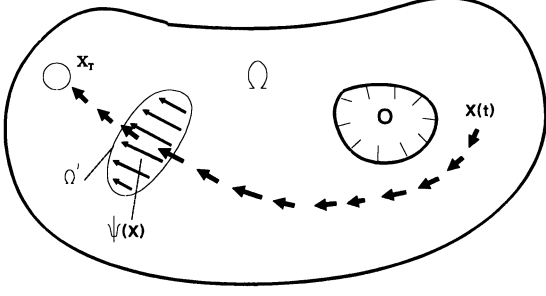


Fig. 7. Domain of a modified HPC.

In this work, the modified HPC is required to synthesize the control signal (Fig. 7)

$$U = -\nabla V(X, \Psi(X), \Gamma, X_T) \quad X \in \Omega \quad (6)$$

such that for a system described by (2)

$$\lim_{t \rightarrow \infty} X(t) \rightarrow X_T$$

$$X(t) \cap O \equiv \phi \quad \forall t, \text{ and } \dot{X}^t \Psi(X) > 0 \quad X \in \Omega', \quad \forall t. \quad (7)$$

For convenience, in the remainder of the paper, $V(X)$ is used to refer to $V(X, \Psi(X), \Gamma, X_T)$.

B. Problem Formulation—EHPC

Let O be a set of *a priori* unknown regions in R^N which the agent is required to avoid, Γ is the boundary of O ($\Gamma = \partial O$), and Ω is the space in which the agent is permitted to operate ($\Omega = R^N - O$). In addition, let Ω' be *a priori* unknown. Let S be a sphere with a radius ρ centered around the location of the agent $X(t)$. S represents the region which the agent's on-board sensors can illuminate at time t

$$S(t) = \{X: \|X - X(t)\| \leq \rho\}. \quad (8)$$

Let Γ_c and Ω_c be the accumulating representations for the avoidance and directional regions, respectively, and let Γ_s and ω_s be the avoidance and directional subregions, respectively, which the sensors of the robot can pick up from the point $X(t)$,

$$\begin{aligned} \Gamma_s(t) &= (S(t) \cap \Gamma) - (S(t) \cap \Gamma_c(t - dt)) \\ \omega_s(t) &= (S(t) \cap \Omega') - (S(t) \cap \Omega'_c(t - dt)), \text{ and} \\ \Gamma_c(t) &= \Gamma_c(t - dt) \cup \Gamma_s(t) \\ \Omega'_c(t) &= \Omega'_c(t - dt) \cup \omega_s(t). \end{aligned} \quad (9)$$

Let Q be a time function whose range is restricted to a value from the binary set $\{0, 1\}$. Its value depends on the activities registered by the local sensors such that

$$Q = \begin{cases} 0, & \Gamma_s \in \phi \text{ and } \omega_s \in \phi \\ 1, & \text{Else.} \end{cases} \quad (10)$$

The agent reacts to the transition at t_i of Q from 0 to 1 by modifying its control so that a reverse transition of Q from 1 to 0 occurs at t'_i . The control at t'_i is denoted by the vector field $u_i = -\nabla V_i(X, X_T, Q, V_{i-1})$. For the generation of a successful control action, the agent is required to synthesize a finite

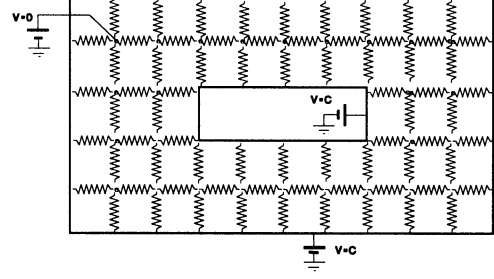


Fig. 8. Resistive grid equivalence of a harmonic planner.

set of successively dependent V_i 's $\{V_i: i = 1, \dots, L < \infty\}$ so that for the gradient dynamical system

$$\begin{aligned} \dot{X} &= -\nabla V_i(X, T, Q, V_{i-1}) \quad X(0) \in \Omega \\ \lim_{i \rightarrow L} X(t) &\rightarrow X_T \quad V_0 = V(X, \Gamma_c(0), X_T) \\ i &\in [1, \dots, L] \\ t &\rightarrow \infty, \quad t \in [t_0, \dots, \infty) \end{aligned} \quad (11)$$

also $X(t) \cap O \equiv \phi$ and $\Psi^t(X) \dot{X} > 0 \quad \forall t.$

IV. PHYSICAL METAPHOR

In this section, a physical metaphor is developed to aid in the derivation of the BVP needed for constructing an HPC that encodes both directional and regional avoidance constraints in the differential properties of the PF. The encoding is done so that the motion generated by the corresponding gradient dynamical system satisfies the conditions in (7).

Analogy with natural processes is an important and powerful tool for problem solving [78]. A proper analogy between a well-understood natural process and the problem at hand may serve as a feasible alternative to the arduous task of mathematically deriving a provably-correct solution to a problem. The HPF approach to motion planning lends itself to this mode of problem solving. It is well known that a path generated by the gradient dynamical system from an HPF in the Dirichlet setting is analogous to the path marked by the electric current moving in a resistive grid (Fig. 8) with the potential set to a positive constant value at the nodes marking the boundary of the forbidden regions and to zero at the node that is located on the target point [32], [33], [51], [53]. The correctness of such an analogy may be easily deduced by discretizing the 2-D Laplacian operator (similar treatment can be applied to dimensions greater than two)

$$\nabla^2 V(x, y) = \frac{\partial^2 V(x, y)}{\partial x^2} + \frac{\partial^2 V(x, y)}{\partial y^2} \quad (12)$$

in order to construct the difference equation

$$\begin{aligned} V(i, j) &= \frac{1}{4} [v(i, j+1) + v(i, j-1) \\ &\quad + v(i+1, j) + v(i-1, j)]. \end{aligned} \quad (13)$$

Equation (13) may be interpreted as an element with four equal resistors ($R = 1$) connected to a node with a $V(i, j)$ voltage (Fig. 9).

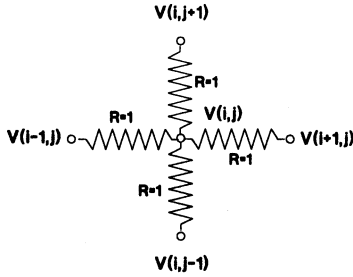
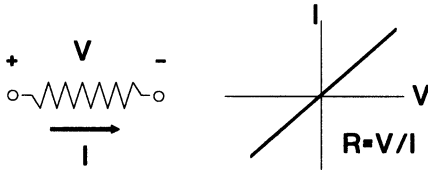
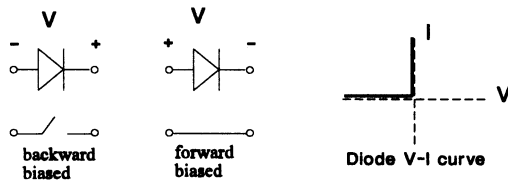


Fig. 9. Resistive element used in constructing a harmonic potential.

Fig. 10. $V-I$ characteristics of a linear resistor.Fig. 11. $V-I$ characteristics of an ideal diode.

As can be seen, in the harmonic approach, a resistive element is the one manipulating the electric current or, equivalently, the motion of the agent. A resistor is a linear, bilateral electric component with characteristics that remain unchanged, regardless of the direction the current assumes inside the element (Fig. 10).

To add the needed directional sensitivity, an electric element that is sensitive to the direction of the current needs to be used along with the resistive element for building a grid that would manipulate the flow of the electric current in the desired manner. The new element is a diode [79]. Ideally, a diode is a voltage-controlled switch that can be in either one of two states (Fig. 11): either a forward-biased state, in which its resistance is zero, or backward-biased, in which the resistance is infinite.

A more realistic model of a diode is that of a resistive element whose resistance (R_d) remains finite but varies depending on the direction in which the current flows (Fig. 12):

$$R_d = \begin{cases} R_f & \text{if forward biased} \\ R_b & \text{if backward biased} \end{cases}$$

where $R_b \gg R_f$.

A diode and a resistor are sufficient elements for building a grid that would control the flow of the electric current in a manner that is analogous to the behavior of the suggested planner. In the regions of the workspace marked as free traffic zones ($\Omega - \Omega'$), a resistive element only is used for building the motion control grid (Fig. 13). In regions where the direction of

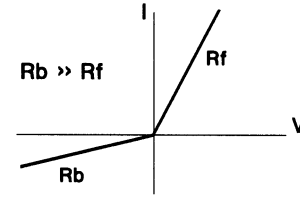
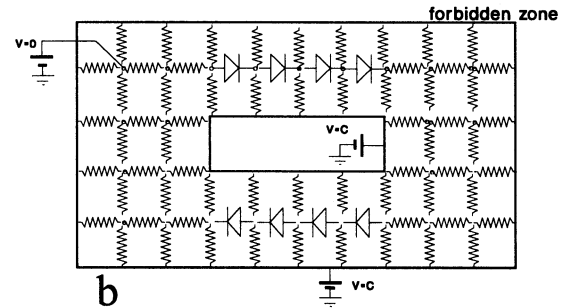
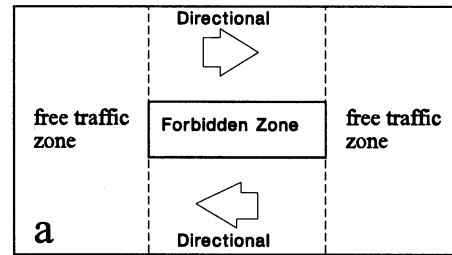
Fig. 12. $V-I$ characteristics of a realistic diode.

Fig. 13. (a) Environment with directional and regional avoidance constraints. (b) Electric grid with diodes and linear resistors used to generate the potential whose gradient can generate motion that enforce both types of constraints.

traffic is constrained (Ω'), a diode element is used in the construction of the grid so that it is placed in a backward-biased mode along the inadmissible direction of traffic. The voltage of the nodes marking the boundary of the forbidden regions is set to a constant, positive voltage, and the voltage of the node marking the target is set to zero.

V. NONLINEAR, ANISOTROPIC, NAVIGATION FIELD SYNTHESIS

Based on the metaphor suggested in Section III, the modified BVP that is capable of encoding both directional and regional avoidance constraints is derived.

A. Modified Differential Operator

An HPF is constructed by forcing the divergence ($\nabla \cdot$) of the gradient of the PF, which is analogous to the electric current in a resistive grid, to zero inside Ω

$$\nabla \cdot \nabla V(X) = \nabla^2 V(X) \equiv 0 \quad X \in \Omega. \quad (14)$$

This condition guarantees the continuity of the current, which in turn guarantees the continuity of motion, inside Ω . As a result, deadlock is prevented and motion is steered to the global minimum of $V(X)$, which is situated on X_T . As can be seen, by choosing the Laplacian operator as the governing relation

of the differential behavior of the electric current (i.e., motion), no preferable direction for motion to proceed along can be encoded in the behavior of the agent (i.e., the workspace is linear and isotropic). To modify the governing differential operator so that along with guaranteeing the continuity of motion inside Ω , favorable directions of motion inside Ω' may also be enforced, the metaphor in Section III is used. At a point $X \in \Omega'$, an infinitesimal diode is assumed to be present and oriented in a manner such that the favorable direction of motion, which is marked by the vector $\Psi(X)$, coincides with the direction in which the diode is in a forward-biased mode. This means that the current experiences low resistance R_f , or equivalently high conductance σ_f , along that direction. On the other hand, the current experiences high resistance R_b , or equivalently low conductance σ_b , along the opposite direction. Therefore, the electric current inside Ω' may be expressed as

$$-\Sigma(X)\nabla V(X) \quad (15)$$

where

$$\Sigma(X) = \begin{bmatrix} \sigma_{x1}(X) & 0 & \dots & 0 \\ 0 & \sigma_{x2}(X) & \dots & 0 \\ \vdots & \vdots & \ddots & \vdots \\ 0 & 0 & \dots & \sigma_{xN}(X) \end{bmatrix}$$

and

$$\sigma_{xi}(X) = \begin{cases} \sigma_f & -\nabla V(X)^t \Psi(X) > 0 \\ \sigma_b & -\nabla V(X)^t \Psi(X) \leq 0 \end{cases} \quad i = 1, \dots, N$$

$\sigma_f \gg \sigma_b$. After sensitizing the electric current to a favorable direction of motion, the continuity constraint is applied by forcing the divergence of the current to be identically zero inside Ω'

$$\nabla \cdot [\Sigma(X) \nabla V(X)] \equiv 0 \quad X \in \Omega'. \quad (16)$$

B. Modified BVP

A BVP, which may be used to generate a PF for constructing the gradient control signal in (6) that is capable of enforcing the regional avoidance and the directional constraints, is the following: solve

$$\nabla^2 V(X) \equiv 0 \quad X \in \Omega - \Omega'$$

$$\text{and } \nabla \cdot [\Sigma(X) \nabla V(X)] \equiv 0 \quad X \in \Omega'$$

$$\text{subject to } V(X_T) = 0, \quad V(X)|_{X \in \Gamma} = C. \quad (17)$$

VI. PERFORMANCE VERIFICATION

It may be clear from the analogy in Section III that motion from the gradient dynamical system representing the control signal in (6) will be steered to the target state X_T from any

starting point in Ω in a manner that satisfies both the directional and regional avoidance constraints. However, in the following, a mathematical proof is provided to verify these capabilities. First, it ought to be mentioned that since the BVP in (17) is constructed based on an analogy with a natural process, its solution exists. It can be mathematically shown that the solutions of BVPs connected with the partial differential operator $\nabla \cdot [\sigma(x)\nabla V(x)]$, which includes the BVP in (17), exist. However, the proof is mathematically involved and will not be discussed in this paper. For a proof of existence, see [80]–[82].

A. Differential Operator

The governing partial differential relation in Ω' (13) is re-expressed as

$$\begin{aligned} \nabla \cdot [\Sigma(X) \nabla V(X)] &\equiv 0 \quad X \in \Omega' \\ &= \sum_{i=1}^N \frac{\partial}{\partial x_i} \left(\sigma_{xi}(X) \frac{\partial V(X)}{\partial x_i} \right) \\ &= \sum_{i=1}^N \left[\sigma_{xi}(X) \frac{\partial^2 V(X)}{\partial x_i^2} + \frac{\partial V(X)}{\partial x_i} \frac{\partial \sigma_{xi}(X)}{\partial x_i} \right] \end{aligned} \quad (18)$$

since $\sigma_{xi}(X) = \sigma_b + (\sigma_f - \sigma_b)\Phi(\nabla V(X)^t \Psi(X))$, the above expression becomes (19), shown at the bottom of the page, where $\Phi(\cdot)$ is the unit step function, and $\delta(\cdot)$ is the Dirac-delta function. As can be seen, the second term of (19) is either zero or infinity. Since the solution of the operator subject to the boundary conditions in (17) exists, the value of the differential operator should be zero everywhere in Ω' . Therefore, the governing differential relation may be written as

$$\sum_{i=1}^N \sigma_{xi}(X) \frac{\partial^2 V(X)}{\partial x_i^2} \equiv 0 \quad X \in \Omega' \quad (20)$$

or

$$\sum_{i=1}^N k_i(X) \frac{\partial^2 V(X)}{\partial x_i^2} \equiv 0 \quad X \in \Omega \quad (21)$$

where

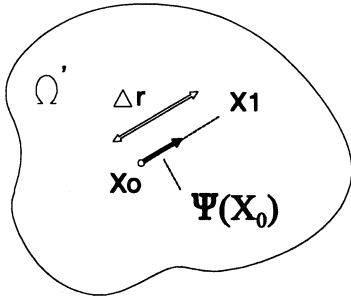
$$k_i(X) = \begin{cases} \sigma_f & X \in \Omega - \Omega' \\ \sigma_{xi}(X) & X \in \Omega'. \end{cases}$$

B. Maximum Principle

Proposition 1: The PF generated by the BVP in (17) assumes its extrema on its boundary.

Proof: If at any point $X \in \Omega$ $V(X) \leq 0$, \exists a local minimum inside Ω such that $\partial^2 V(X)/\partial x_i^2 > 0$. Since all $k_i(X)$'s are positive, (21) will be violated. Therefore, $V(X)$ should be greater than zero for all $X \in \Omega$. In a similar way, if at any point $X \in \Omega$ $V(X) \geq C$, \exists a local maximum inside Ω such that

$$= \sum_{i=1}^N \left[\sigma_{xi}(X) \frac{\partial^2 V(X)}{\partial x_i^2} + (\sigma_f - \sigma_b) \delta(\nabla V(X)^t \Psi(X)) \frac{\partial V(X)}{\partial x_i} \frac{\partial V(X)^t \Psi(X)}{\partial x_i} \right] \quad (19)$$

Fig. 14. Point inside Ω' .

$\partial^2 V(X)/\partial x_i^2 < 0$. Therefore, the value of $V(X)$ cannot be equal to or exceed C in Ω . In other words, $V(X)$ assumes its maximum and minimum on its boundary.

C. Uniqueness of the Potential

Proposition 2: There is one and only one solution to the BVP in (17).

Proof: Let us assume that there are two solutions $(V1, V2)$ to (17) in Ω . Let DV be the difference between these two solutions $DV = V1 - V2$. It ought to be noticed that DV is also a solution to (17). Proving that DV vanishes everywhere in Ω proves that the solution is unique.

Let Γ_T be the boundary of an infinitesimal circle surrounding X_T on which the potential of $V1$ and $V2$ is set to zero. In addition, $V1$ and $V2$ are forced to have equal positive constant values on Γ . In other words, DV is identically zero on the boundary of Ω . As a result of the maximum principle, DV is zero everywhere in Ω . This proves the uniqueness of solution of the BVP in (17).

D. Satisfaction of the Directional Constraints

Proposition 3: For any point $X \in \Omega'$, $\dot{X}^t \Psi(X) > 0$.

Proof: Let X_0 be a point inside Ω' (Fig. 14). Let X_1 be another point in that region constructed by extending X_0 a small distance (Δr) along the direction of the unit vector $\Psi(X_0)$, i.e., $X_1 = X_0 + \Psi(X_0)\Delta r$.

By integrating the partial differential relation in (20) along the $\Psi(X_0)$ direction, one can approximate the potential at X_1 as

$$\begin{aligned} V(X_1) &\approx V(X_0) + \frac{k}{\sigma_{x_i}(X_0)} \|\nabla V(X_0)^t \Psi(X_0)\| \Delta r \\ &= V(X_0) + \frac{k}{\sigma_{x_i}(X_0)} \left\| \frac{\partial V(X_0)}{\partial \Psi(X_0)} \right\| \Delta r \end{aligned} \quad (22)$$

where k is a finite positive constant. Let us assume that the directional constraints are violated, i.e.,

$$\dot{X}^t \Psi(X_0) \leq 0, \quad X_0 \in \Omega'. \quad (23)$$

Note that $\dot{X} = -\nabla V(X)$. There are two possibilities:

1) $\dot{X}^t \Psi(X_0) = 0$. Here, the second term of (19), i.e.,

$$\sum_{i=1}^N (\sigma_f - \sigma_b) \delta(\Delta V(X)^t \Psi(X)) \frac{\partial V(X)}{\partial x_i} \frac{\partial \nabla V(X)^t \Psi(X)}{\partial x_i} \quad (24)$$

will become infinite, making the relation in (20) impossible to satisfy. This possibility is already ruled out by the fact that the solution of the suggested BVP exists.

2) $\dot{X}^t \Psi(X_0) < 0$. For this case, $\sigma_{x_i}(X_0) = \sigma_b$. When constructing the NAHPF, σ_b is chosen to be a very small positive number ($\sigma_b \ll 1$). This results in a high value for $V(X_1)$ that will exceed the value of the potential at Γ , i.e., $V(X_1) \gg C$. This possibility is ruled out since it leads to the violation of the maximum principle.

As can be seen, the only remaining possibility is that $\dot{X}^t \Psi(X_0) > 0$, $X_0 \in \Omega'$. In other words, the directional constraints must be satisfied.

E. PF Generated by (17) Is an HPF

Proposition 4: Within the context of the BVP in (17), the partial differential operator

$$\sum_{i=1}^N k_i(X) \frac{\partial^2 V(X)}{\partial x_i^2} \equiv 0 \quad X \in \Omega \quad (25)$$

reduces to the simple Laplacian operator

$$\sum_{i=1}^N \frac{\partial^2 V(X)}{\partial x_i^2} \equiv 0 \quad X \in \Omega. \quad (26)$$

Proof: This simply follows from Proposition 3. Since directional constraints are satisfied for every point in Ω' , $\sigma_{x_i}(X) = \sigma_f \forall X \in \Omega'$, i.e.,

$$k_i(X) = \begin{cases} \sigma_f, & X \in \Omega - \Omega' \\ \sigma_f, & X \in \Omega' \end{cases} \quad (27)$$

which reduces (25) to

$$\sum_{i=1}^N \sigma_f \frac{\partial^2 V(X)}{\partial x_i^2} \equiv 0 \quad X \in \Omega \quad (28)$$

or, equivalently, to

$$\sum_{i=1}^N \frac{\partial^2 V(X)}{\partial x_i^2} \equiv 0 \quad X \in \Omega$$

which is the well-known Laplacian operator. In other words, $V(X)$ is an HPF.

F. Satisfaction of the Regional Avoidance Constraints

Proposition 5: If $X(0) \in \Omega$, the motion steered by the gradient dynamical system in (6) will always remain inside Ω (i.e., $X(t) \cap O \equiv \phi \forall t$).

Proof: Consider the part of Ω near an obstacle O (Fig. 15). Let $n(X)$ be a vector that is normal to the surface of the obstacle Γ , $X \in \Gamma$. Let O' be a region created by infinitesimally expanding the forbidden region O such that $O \subset O'$, and $\Gamma' = \partial O'$. The radial derivative of $V(X)$ along $n(X)$ may be computed as

$$\frac{\partial V(X)}{\partial n(X)} = \frac{V(X') - V(X)}{(X' - X)^t n(X)}, \quad X' \in \Gamma' \quad (29)$$

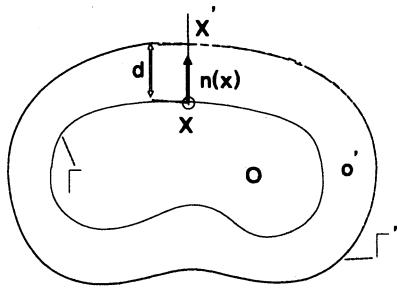


Fig. 15. Region constructed by expanding the boundary of an obstacle.

where X' is taken as the minimum distance between X and Γ' . Since the value of the potential in Ω is less than C , and X' lies inside Ω , the radial derivative of the potential along $n(X)$ is negative

$$\frac{\partial V(X)}{\partial n(X)} < 0. \quad (30)$$

Let us assume that $X(t)$ is initially located at X' , and d is the distance between $X(t)$ and X

$$d = n(X)^t (X(t) - X). \quad (31)$$

Note that since X' is initially inside Ω , d is initially positive. Let L be a measure of that distance

$$L = d^2. \quad (32)$$

Noting that $n(X)$ is not a function of time, and $\partial V/\partial n = n^t \nabla V$, the rate of change of L with respect to time may be computed as

$$\begin{aligned} \frac{dL}{dt} &= 2d\dot{d} = 2dn^t(X)\dot{X}(t) = -2dn^t(X)\nabla V(X) \\ &= -2d\frac{\partial V(X)}{\partial n(X)} > 0. \end{aligned} \quad (33)$$

Therefore d is increasing with time and $X(t)$ is being steered away from Γ . This makes it impossible for $X(t)$ to intersect O at any time, i.e.,

$$X(t) \cap O \equiv \emptyset \quad \forall t. \quad (34)$$

G. $V(X)$ Is a Lyapunov Function Candidate

The aim of this work is for it to be a step toward designing an intelligent controller that would sensitize an agent in a constrained, goal-oriented manner to its surroundings. Such a task entails the ability of the control device to fuse AI capabilities with classical control action. Until recently the setting for constructing such controllers has remained reliant on an HLC that utilizes classical or evolutionary AI techniques to convert the goal of the agent, the constraints on its behavior, and the data about its environment into a sequence of reference commands which are in turn fed to a classical LLC whose function is to generate a control signal enabling the robot to follow the reference set by the HLC [Fig. 16(a)]. One shortcoming of the

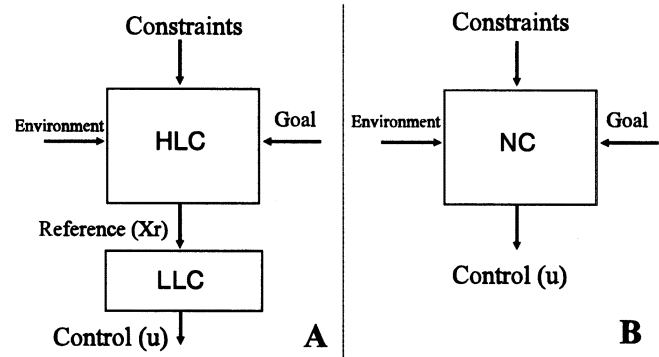


Fig. 16. Settings for intelligent controllers. (a) HLC-LLC setting. (b) Navigation control.

forementioned setting is the lack of guarantees that the HLC generated reference can be converted into a successful control action by the LLC. Recently, a new class of controllers called navigation control (NC) was suggested to get around this difficulty [77]. Such controllers aim at integrating the functions of both the HLC and LLC in one control module, therefore eliminating the potential for conflict [Fig. 16(b)]. Instead of using rigid, whole-domain control functions that are unequipped to comply with the stringent behavioral constraints an agent requires for successful purposive behavior, the control action in an NC is induced on a PF surface. Therefore to accommodate the manner in which an NC functions, the potential field must have a dual nature: one that is related to AI, while the other is related to classical control.

As was briefly discussed at the beginning of this paper and with some details in [70]–[72], the potential field ($V(X)$) may be viewed as an evolutionary, intelligent, AL machine. Here, we show that $V(X)$ is also a Lyapunov function candidate (LFC.) Lyapunov's method [83], [84] is the leading tool for the analysis of nonlinear control systems. By proving that $V(X)$ is also an LFC, the dual nature of this group of PFs is established, hence, its usability for constructing an NC.

1) *Lyapunov's Method:* In order for the system

$$\dot{X} = f(X) \quad (35)$$

to be globally asymptotically stable (i.e., $\lim_{t \rightarrow \infty} X(t) \rightarrow X_T$), it is sufficient that there exists a scalar function $V(X)$ with continuous first partial derivatives with respect to X so that

$$\begin{aligned} \text{a) } & V(X) = 0 \quad X = X_T \\ \text{b) } & V(X) > 0 \quad X \neq X_T \\ & \text{(i.e., } V(X) \text{ is positive definite)} \end{aligned} \quad (36)$$

and for $\dot{V}(X) = (\partial V(X)/\partial t)$

$$\begin{aligned} \text{c. } & \dot{v} = 0 \quad X = X_T \\ \text{d. } & \dot{v} < 0 \quad X \neq X_T, \quad [\text{i.e., } V(X) \text{ is negative definite}]. \end{aligned}$$

A $V(X)$ that satisfies *a* and *b* is called an LFC. If $V(X)$ satisfies all of the above conditions, it is called an LF. Usually, another condition for $V(X)$ to be a LF is for $V(X) \rightarrow \infty$ with $\|X\| \rightarrow \infty$. However, since we are dealing with finite domains, this condition is not applicable.

Proposition 6: The potential field $V(X)$, which is generated by the BVP in (17), is an LFC.

Proof: Since by construction $V(X_T) = 0$, showing that $V(X)$ is an LFC requires only showing that $V(X) > 0 \forall X \in \Omega$. This directly follows from the maximum principle. Therefore, $V(X)$ is an LFC.

H. Convergence

To examine the convergence of motion from any point in Ω to X_T , a variation of the Lyapunov method called the LaSalle theorem [88] is needed. This theorem is stated below for convenience.

Theorem: Assume that for the dynamical system

$$\dot{X} = f(X) \quad (37)$$

there exists the scalar function $V(X)$ such that

$$\begin{aligned} V(X) > 0 \quad \forall X \neq X_T, \quad V(X_T) = 0, \quad \text{and} \\ \frac{dV(X)}{dt} \leq 0 \quad \forall X. \end{aligned} \quad (38)$$

Let E be the set of all points where $dV(X)/dt = 0$, and let M be the largest invariant set contained in E . Then, every solution of the above system bounded for $t \geq 0$ approaches M as $t \rightarrow \infty$.

Proposition 7: The motion generated by the control signal in (6) will globally and asymptotically converge to X_T

$$\lim_{t \rightarrow \infty} X(t) \rightarrow X_T \quad \forall X(0) \in \Omega. \quad (39)$$

Proof: From the maximum principle, it is obvious that $V(X)$ is an LFC, i.e., $V(X) > 0 \forall X \neq X_T, V(X_T) = 0$. As for the time derivative of V , it may be computed as

$$\dot{V} = \nabla V(X)^t \dot{X}(t) = -\nabla V(X)^t \nabla V(X) = -\|\nabla V(X)\|. \quad (40)$$

Since it was shown that the dynamical system in (6) can only generate solution trajectories that are bounded to Ω , the zeros of the gradient of $V(X)$ ($\nabla V(X)$) are the ones that determine convergence.

The value of $\nabla V(X)$ is zero in the following cases.

- 1) By design, the gradient dynamical system (6) has a stable equilibrium point at the target location.
- 2) In [85], Koditschek showed that the gradient field of a scalar potential contains at least one zero-measure set (π) of unstable equilibrium.
- 3) An unstable equilibrium zone may form on a subset (Γ'_b) of the interface between the nonlinear, anisotropic region and the rest of the workspace (Γ').

While $E = \{X_T\} \cup \{\pi\} \cup \{\Gamma'_b\}$, the largest invariant set M consists of the only stable equilibrium subset of E ($M = \{X_T\}$.) Therefore, the motion of the gradient system in (6) will converge to X_T .

I. Optimality

Proposition 8: The control action generated by the gradient dynamical system in (6) from the underlying PF of the BVP in (17) is optimal.

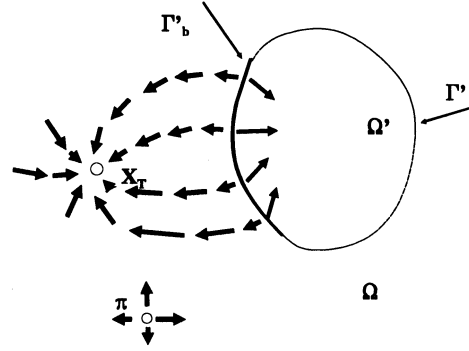


Fig. 17. Gradient field configurations of an NAHPF.

Proof: Let us construct the following energy functional from the control signal in (6):

$$\begin{aligned} J &= \int_{\Omega} \int u^t u d\Omega = \int_{\Omega} \int \nabla V(X)^t \nabla V(X) d\Omega \\ &= \int_{\Omega} \int \sum_i \left(\frac{\partial V(X)}{\partial x_i} \right)^2 dx_1 \dots dx_i \dots dx_N. \end{aligned} \quad (41)$$

The above functional is well known in the calculus of variations. It is called the Dirichlet integral. It is also a well-known result that this functional is globally minimized if $V(X)$ satisfies Laplace's equation (see [86, pp. 18] and [87, pp. 17]). This is called the Dirichlet principle. Since the control action (6) is derived from the gradient of a potential that satisfies the Laplace equation, it minimizes the above energy functional. In other words, the control is optimum.

VII. SIMULATION RESULTS

The following simulation examples are intended to highlight some of the properties of the suggested method. They also demonstrate the diversity of applications the method can handle.

A. HPF Versus NAHPF

It is not hard to see that the behavior an NAHPF-based HPC is capable of projecting subsumes that of an HPF-based HPC (Fig. 17). While there are salient similarities in behavior from both HPC forms, there are, nevertheless, profound differences that are not amenable to analysis or interpretation within the framework of HPFs. The following example is intended to highlight some of these differences. An environment similar to the one in Fig. 13 is chosen for this test. It consists of three different types of domains:

- 1) forbidden regions;
- 2) constrained-traffic regions;
- 3) free-traffic regions.

The forbidden region is $O = O1 \cup O2$, $O1 = \{40 \leq x \leq 0, 40 \leq y \leq 0\}$, $\Gamma1 = \{40 \leq x \leq 0, y = 0\} \cup \{40 \leq x \leq 0, y = 40\} \cup \{x = 0, 40 \leq y \leq 0\} \cup \{x = 0, 40 \leq y \leq 40\}$, $O2 = \Gamma2 = \{8 \leq x \leq 32, y = 20\}$. The constrained-traffic region is $\Omega' = \Omega1' \cup \Omega2'$, $\Omega1' = \{8 \leq x \leq 32, 20 \leq y \leq 40\}$, $\Psi1(x, y) = [x/|x|0]^t x, y \in \Omega1', \Omega2' \{8 \leq x \leq 32, 0 \leq y \leq$

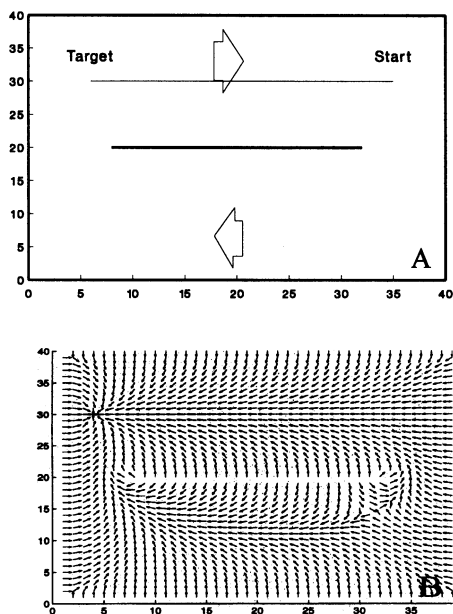


Fig. 18. HPF-based HPC. (a) Generated trajectory. (b) Corresponding, navigation, gradient field.

20}, $\Psi_2(x, y) = [-x/|x| \ 0]^t$, $x, y \in \Omega_2'$. The free-traffic zones are $\Omega_1 = \{0 \leq x \leq 8, 0 \leq y \leq 40\}$, $\Omega_2 = \{32 \leq x \leq 40, 0 \leq y \leq 40\}$. The target point is $(x_T = 5, y_T = 35)$, and the starting point is $(x(0) = 35, y(0) = 35)$. In other words, the environment consists of two unidirectional lanes where the agent can only switch lanes at either the beginning or the end of the road without crossing a forbidden region. First, the HPF-based planner is tested.

The potential is generated by solving the BVP

$$\frac{\partial^2 V(x, y)}{\partial x^2} + \frac{\partial^2 V(x, y)}{\partial y^2} = 0 \quad x, y \in \Omega_1 \cup \Omega_2 \cup \Omega_1' \cup \Omega_2' \quad (42)$$

subject to

$$V(x_T, y_T) = 0, \quad V(x, y)|_{x, y \in \Gamma} = C.$$

As can be seen from Fig. 18(a), the planner totally disregarded the directional constraints and drove the state along the shortest path (a straight line) to the target. The corresponding gradient navigation field is shown in Fig. 18(b). The NAHPF field is generated by solving the BVP

$$\begin{aligned} \frac{\partial^2 V(x, y)}{\partial x^2} + \frac{\partial^2 V(x, y)}{\partial y^2} &= 0 \quad x, y \in \Omega_1 \cup \Omega_2 \\ \sigma_x(x, y) \frac{\partial^2 V(x, y)}{\partial x^2} + \sigma_y(x, y) \frac{\partial^2 V(x, y)}{\partial y^2} &\equiv 0 \\ &x, y \in \Omega_1' \cup \Omega_2' \end{aligned}$$

subject to $V(x_T, y(T)) = 0, \quad V(x, y)|_{x, y \in \Gamma} = C.$ (43)

The path generated by the modified planner is shown in Fig. 19(a), and the corresponding gradient field is shown in Fig. 19(b). As can be seen, the gradient field from the modified potential successfully steered the state toward the target avoiding the forbidden regions and enforcing the directional

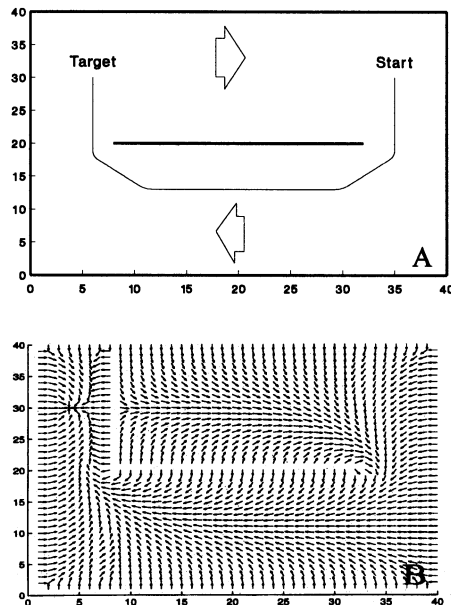


Fig. 19. NAHPF-based HPC. (a) Generated trajectory. (b) Corresponding, navigation, gradient field.

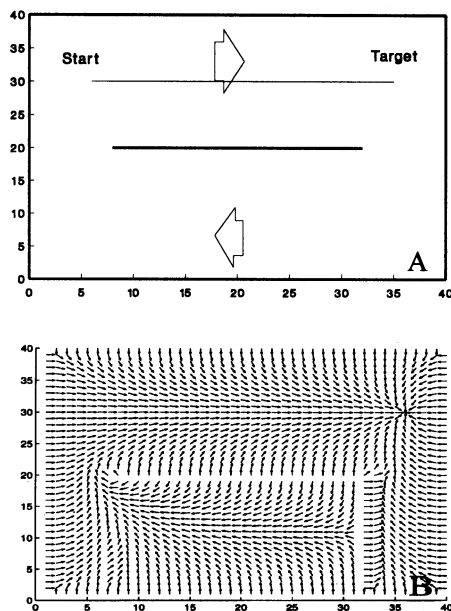


Fig. 20. NAHPF-based HPC. (a) Generated trajectory. (b) Corresponding, navigation, gradient field.

constraints. In Fig. 20(a), the target and starting points are interchanged, i.e., $(x_T = 35, y_T = 35)$, $(x(0) = 5, y(0) = 35)$. As can be seen, the modified planner drove the state along a straight line to the target as if it were being steered by a linear, harmonic planner. The steering gradient field is shown in Fig. 20(b).

Although from a first casual look the gradient field of the NAHPF may appear similar to that of the HPF, the fact is that the gradient of the modified potential possesses unique structural properties that are significantly different from those of a gradient field generated from the HPF. Consider, for example,

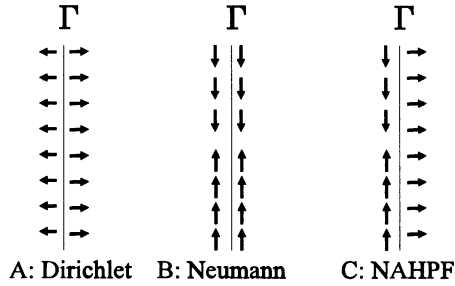


Fig. 21. Field configuration around the boundary of an obstacle.

the field from the NAHPF in Fig. 19(b) in comparison with that from the HPF in Fig. 18(b), in particular, the vertical straight line pattern that appears at the left corner of the upper corridor in the modified field [Fig. 19(b)]. It may appear as if the field from the modified potential is obtained by adding a boundary condition at $\{x = 8, 20 \leq y \leq 40\}$ and solving a linear harmonic BVP similar to the one in (42). In the following, the fallacy of this assumption is proven. There are two basic settings in which boundary conditions can be applied to a harmonic BVP:

- 1) a homogeneous, Dirichlet boundary conditions in which the value of the potential at the boundary is kept constant, i.e., $V(X) = CX \in \Gamma$;
- 2) a homogenous Neumann boundary conditions in which the radial derivative of the potential is set to zero $\partial V(X)/\partial n = 0, X \in \Gamma$.

It is possible to use combinations of the above two to generate other boundary conditions. Since in the first case the voltage is kept constant along the boundary, the gradient along the tangent to the boundary is zero (i.e., $\partial V(x)/\partial t = 0, X \in \Gamma$). In other words, for this case, the gradient field can only be projected normal to Γ [Fig. 21(a)]. For the homogeneous Neumann case, the choice of the boundary condition forces the radial component of the gradient field along Γ to zero. Therefore, in a situation where the Neuman setting is present, the gradient field has to be tangent to the boundary [Fig. 21(b)]. It is not hard to see that the two settings are mutually exclusive in the sense that the presence of one field pattern at any side of the boundary immediately excludes the presence of the other field pattern on the other side. Now let us examine the structure of the gradient field around both sides of the line pattern in Fig. 19(b). At one side of the line, the gradient field is normal to Γ , and at the other side, a component of the gradient field is tangent to Γ [Fig. 21(c)]. As can be seen, attempting to attribute the appearance of the above straight line pattern in the gradient field of the NAHPF to an added boundary condition will immediately lead to a logical contradiction.

Another point in which the structure of the gradient field from the modified potential departs from that of a linear harmonic potential, or any linear potential for that matter, has to do with the nature of the critical points of the field. In [85], Koditschek showed that the construction of a PF (the class of fields that was considered being scalar fields) with a gradient that does not vanish anywhere in Ω , except at the target point, is impossible. Zones of zero measures (i.e., points) will always be present in the gradient at which the field vanishes. However those re-

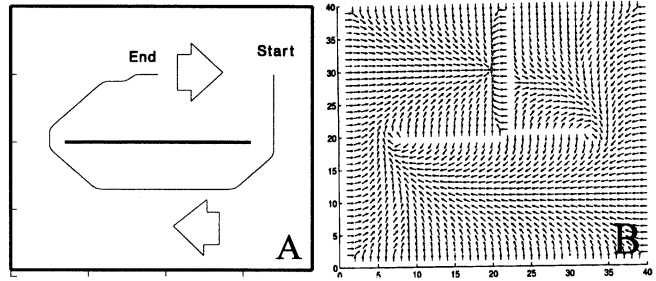


Fig. 22. NAHPF-based HPC, target inside the nonlinear anisotropic region. (a) Generated trajectory. (b) Corresponding, navigation, gradient field.

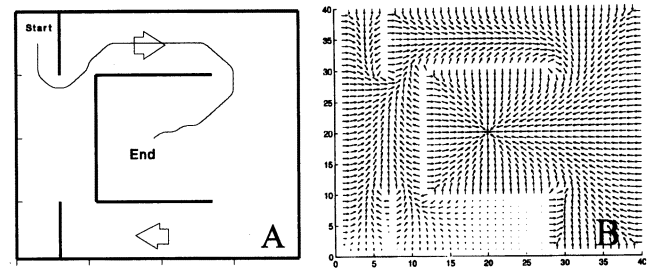


Fig. 23. NAHPF-based HPC, a more complex environment. (a) Generated trajectory. (b) Corresponding, navigation, gradient field.

gions constitute no danger of trapping motion before it reaches the target, due to their unstable nature. The presence of such points is easily detectable in the linear, harmonic gradient field in Fig. 18(b) (right upper corner of the bottom corridor). This result no longer holds for the class of NAHPFs introduced in this paper. Earlier in this section, it was shown that it is impossible for the line pattern appearing in the field in Fig. 19(b) to have been caused by the addition of a boundary condition. This leaves the only possibility that the line pattern in Fig. 19(b), which constitutes an unstable equilibrium zone of zero width, but finite height, is inherent in the structure of the gradient fields generated by the NAHPF. These zones are no longer a set of isolated points.

B. More Examples—NAHPF

In Fig. 22, the target was placed inside the nonlinear, anisotropic region of the space. As can be seen, the planner functioned as expected enforcing both directional and regional avoidance constraints. Fig. 22(a) shows the trajectory laid by the planner, whereas Fig. 22(b) shows the corresponding gradient, navigation field.

In Fig. 23, the planner is presented with a more complex environment. Fig. 23(a) shows the laid trajectory, and Fig. 23(b) shows the corresponding gradient navigation field. It can be seen that NAHPFs suffer from the same vanishing field problem as their HPF counterparts. In [50], the authors introduced biharmonic potential fields as an alternative that does not suffer from this problem. The authors hope to be able to extend the biharmonic approach to accommodate nonlinear, anisotropic spaces.

In the above example, the planner is assumed to *a priori* know the constraints on motion (i.e., the avoidance and directionally-constrained regions). In the following example, this information

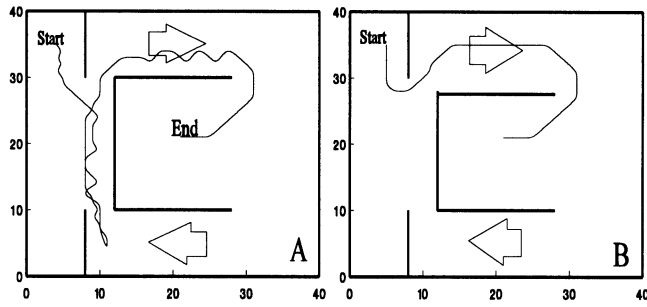


Fig. 24. Trajectories generated by an NAHPF-based EHPC. (a) First attempt. (b) Second attempt.

is not *a priori* available to the planner. The target location is the only piece of information that is *a priori* known. To plan under such conditions, the NAHPF is configured in an EHPC mode where partial information about the environment is fed online to the controller and used to evolve the control policy. Fig. 24 shows the trajectories laid by the EHPC, NAHPF-based controller in an environment similar to the one in Fig. 23(a). The controller proceeds with guiding the agent totally oblivious to the presence of the avoidance and traffic-regulated regions [Fig. 24(a)]. Each time a constraint is discovered, the controller integrates it in its database and then modifies the control policy. Although the agent wanders a little at the first attempt, it does not violate any constraint and succeeds in reaching the target. Equipped with the knowledge it gained from the first attempt, the controller is utilized in a second attempt to guide the agent to the target [Fig. 24(b)]. As can be seen, the controller eliminates all unnecessary detours from the path, significantly enhancing the quality of the trajectory and shortening the distance traveled.

C. Di-Graphs

The NAHPF-based controller has special significance when Ω is discretized. In a discretized workspace, motion of the state is limited to a web of infinitesimal passages. This situation is analogous to a graph where a passage resembles an edge of a graph and a junction in the web represents a vertex in the graph. NAHPFs make it possible to tackle an important class of graphs called directed-graphs. Unlike regular graphs where bilateral transitions between vertices are allowed, the cost of a transition from one vertex in a di-graph to another differ from that of the reverse transition.

The cost assigned to an edge is analogous to the resistance of the corresponding passage. This is represented as a lumped resistive element connecting the corresponding vertices [Fig. 25(a)]. As for a di-graph, the cost associated with the edges marking the forward and reverse transitions between two vertices are analogous to the forward and backward resistances of a diode [Fig. 25(b)]. As was mentioned at the beginning of this paper, the problem of finding the least cost path linking two vertices in a di-graph is an important problem in operations research. Motivated by the physical fact that the highest value of an electrical current between two points tends to flow along the minimum resistance (or equivalently, minimum cost) path, the authors believe that there is a strong possibility that the suggested NAHPF-based control scheme can be used to solve this problem. The following conjecture is an expression of this possibility.

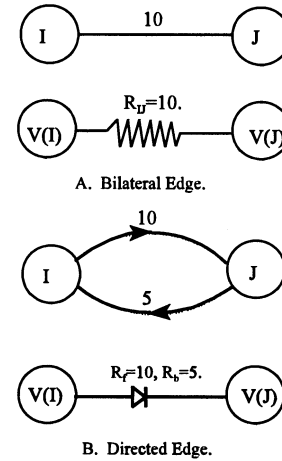


Fig. 25. Graph components and their analogous electric components.

Conjecture 1: Let G be a directed graph, N a set of vertices, Z the corresponding set of edges, N_I the initial vertex, and N_T the target vertex. Assume that at each vertex N_i , there is a voltage $V(N_i)$, and the terminal vertices are assigned the values $V(N_I) = 1$, $V(N_T) = 0$. Let the cost of moving between vertices i and j be R_{ij} if the edge is bilateral, and Rd_{ij} if the edge is directed

$$Rd_{ij} = \begin{cases} Rf_{ij}, & V(N_i) > V(N_j) \\ Rb_{ij}, & V(N_i) \leq V(N_j). \end{cases} \quad (44)$$

Assume that every vertex in G is governed by Kirchoff's current law (summation of the currents entering or leaving a vertex is equal to zero [89], i.e., no accumulation of charge is permitted)

$$\Delta I_i = \sum_j \frac{V(N_i) - V(N_j)}{Rt_{ij}} = 0 \quad (45)$$

where $Rt_{ij} = R_{ij}$ if the edge is bilateral, and $Rt_{ij} = Rd_{ij}$ if the edge is directed. This law may be considered as the equivalent to Laplace's equation in discrete domains.

The trajectory (sequence of vertices) that is constructed by traversing the edges with the highest current flowing out of the vertex under consideration starting from N_I and ending with N_T is the minimum cost path connecting N_I to N_T .

The following examples illustrate the application of the NAHPF-based algorithm to solving the minimum path problem in a di-graph. Fig. 26 shows four di-graphs with a different number of vertices (K) and associated costs of transitions. The currents flowing in the edges of a graph are represented using the matrix $I = [I_{ij}]$, where i is the starting vertex from which the current enters, and j is the ending vertex from which the current leaves.

1) $K = 3$ [Fig. 26(a)]:

$$N_I = 1, \quad N_T = 2, \quad \{V_1 = 1, V_2 = 0, V_3 = 0.5\}$$

$$I = \begin{bmatrix} 0.0 & 0.01 & 0.5 \\ -0.01 & 0.0 & -0.5 \\ -0.5 & 0.5 & 0.0 \end{bmatrix}$$

$$\text{path} = 1 \rightarrow 3 \rightarrow 2, \quad \text{cost} = 2.$$

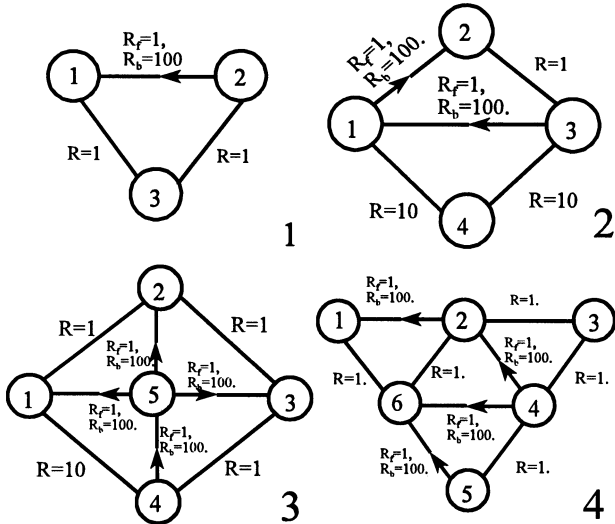


Fig. 26. Different graphs and the corresponding costs of transitions.

2) $K = 4$ [Fig. 26(b)]:

$$N_I = 1, \quad N_T = 3, \quad \{V_1 = 1, V_2 = 0.5, V_3 = 0, V_4 = 0.5\}$$

$$I = \begin{bmatrix} 0.0 & 0.5 & 0.01 & 0.05 \\ -0.5 & 0.0 & 0.5 & 0.0 \\ -0.01 & -0.5 & 0.0 & -0.05 \\ -0.05 & 0.0 & 0.05 & 0.0 \end{bmatrix}$$

path = $1 \rightarrow 2 \rightarrow 3$, cost = 2.

3) $K = 5$ [Fig. 26(c)]: See the first equation at the bottom of the page.

4) $K = 6$ [Fig. 26(d)]: See the second equation at the bottom of the page. To measure the computational complexity of the algorithm suggested in conjecture-1, the scaled CPU execution time of the PC on which simulation was carried out (T_n) is plotted versus the number of vertices of each graph

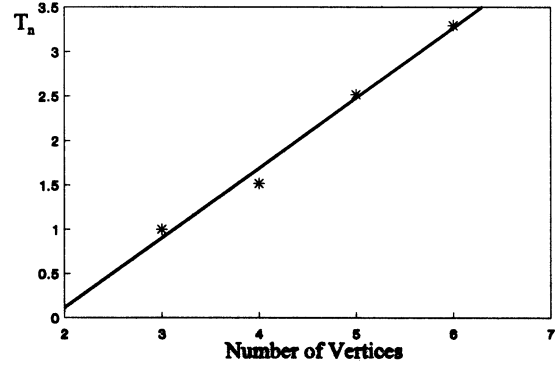


Fig. 27. Scaled CPU execution time versus the number of vertices.

(Fig. 27). The scaling is carried out by dividing the CPU time each simulation took by the time needed to run the simulation for the graph in Fig. 26(a) ($K = 3$). As can be seen, the execution time grows linearly with the number of vertices.

D. Multiagent Motion Planning

A situation where the NAHPF-based control scheme may be applied is multi-robot, multi-target motion planning in a stationary environment (here, a robot is assumed to be a disk with radius d_i). In [90]–[92], the AL approach to behavior synthesis expressed using a hybrid vector-harmonic PF is used for constructing a motion planner of the above type. The planner consists of two components. The first is a component that is constructed for each robot, isolated from the others, to drive each robot to its respective target in a constrained manner. This part of the multiagent controller is referred to as the PRF of the control. The second component of the control functions to mediate any conflict that may arise due to the robots' disregard to each other's presence when constructing their PRFs. This component is called the CRF of the control. The planner is a decentralized,

$$N_I = 1, \quad N_T = 5, \quad \{V_1 = 1, V_2 = 0.7592, V_3 = 0.526, V_4 = 0.2981, V_5 = 0\}$$

$$I = \begin{bmatrix} 0.0 & 0.2408 & 0.0 & 0.0702 & 0.01 \\ -0.2408 & 0.0 & 0.2332 & 0.0 & 0.00759 \\ 0.0 & -0.2332 & 0.0 & 0.2279 & 0.00526 \\ -0.0702 & 0.0 & -0.2279 & 0.0 & 0.00298 \\ -0.01 & -0.00759 & -0.00526 & -0.00298 & 0.0 \end{bmatrix}$$

path = $1 \rightarrow 2 \rightarrow 3 \rightarrow 4 \rightarrow 5$, cost = 4.

$$N_I = 1, \quad N_T = 4, \quad \{V_1 = 1, V_2 = 0.4928, V_3 = 0.2464, V_4 = 0.0000, V_5 = 0.073, V_6 = 0.7390\}$$

$$I = \begin{bmatrix} 0.0 & 0.0051 & 0.0 & 0.0 & 0.0 & 0.2610 \\ -0.0051 & 0.0 & 0.2464 & 0.0049 & 0.0 & -0.2463 \\ 0.0 & -0.2464 & 0.0 & 0.2464 & 0.0 & 0.0 \\ 0.0 & -0.0049 & -0.2464 & 0.0 & -0.0073 & -0.0074 \\ 0.0 & 0.0 & 0.0 & 0.0073 & 0.0 & -0.0073 \\ -0.2610 & 0.2463 & 0.0 & 0.0074 & 0.0073 & 0.0 \end{bmatrix}$$

path = $1 \rightarrow 6 \rightarrow 2 \rightarrow 3 \rightarrow 4$.

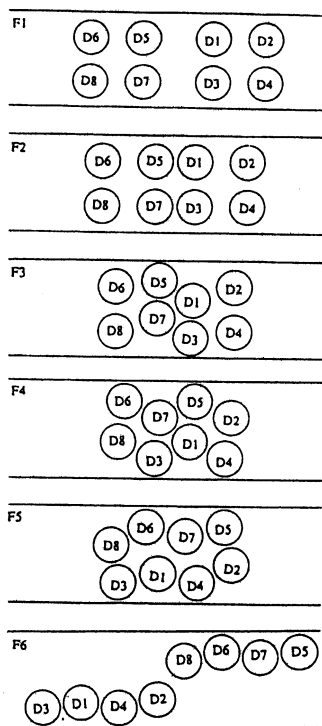


Fig. 28. Collective, decentralized problem solving, multiagent control.

self-organizing machine with a computational complexity that is linear in the number of agents. Moreover, the planner is complete (i.e., if a solution exists, the planner will find it; otherwise it will give an indication that the problem is not solvable) provided that the condition

$$\forall X' \in \Omega \exists X_k \dots X' \in \{X : \|X - X_k\| \leq \rho\} \subset \Omega \quad (46)$$

is satisfied, where $\rho = d'_1 + d'_2$, d'_1 and d'_2 are the radii of the two largest robots in the set of robots occupying the environment. This condition simply means that the narrowest passage in the environment should be large enough to allow any two robots in the group to simultaneously pass each other. In Fig. 28, the capabilities of the multiagent planner are demonstrated. Two groups of four robots each are moving along a road blocking each other's way. The goal is for the two groups to pass each other (i.e., the left group should move to the right, and vice versa for the left group.) The two groups collectively resolved the conflict by forming right and left lanes and confining the motion of each group to one of the lanes.

While condition (46) is by no means stringent (after all, it is only reasonable for a two-way street to be wide enough to allow two vehicles to pass at the same time,) there are nevertheless environments with tight passages that have only room for one robot at a time. In such a situation there are no guarantees that the multiagent planner in [90]–[92] will function properly. One way to remedy this situation is to mark a tight passage as a one-way street (i.e., constrain motion in such passages to become unidirectional.) This may be accomplished by using the NAHPF-based control scheme in synthesizing the PRF control component of the multiagent controller. The following example illustrates the use of NAHPFs for such a purpose.

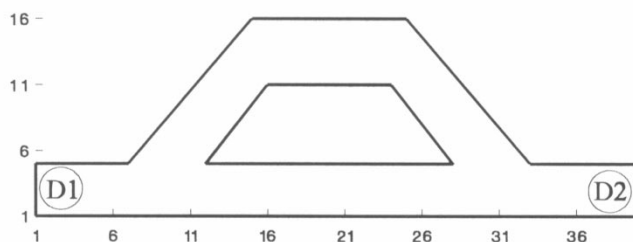


Fig. 29. Workspace with tight passages.

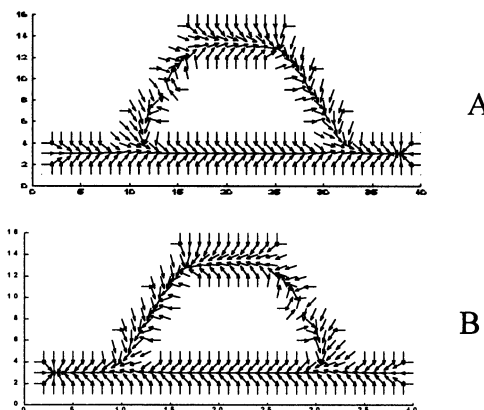


Fig. 30. Gradient fields from an HPF-based HPC. (a) PRF-1. (b) PRF-2.

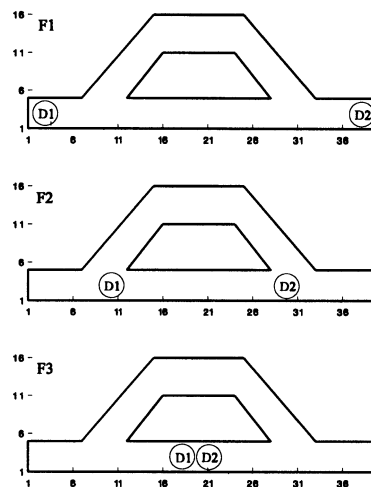


Fig. 31. Failure of an HPF-based, multiagent planner in driving the agents to their targets.

Consider the workspace in Fig. 29. Two robots $D1$ and $D2$ are required to exchange positions. As can be seen, the passages in Ω are not wide enough for the two robots to pass at the same time.

Fig. 30(a) and (b) shows the HPF-based PRFs for both $D1$ and $D2$. Fig. 31 shows, using snapshots, the locations of the robots that are generated by the multiagent controller at different instants of the solution. As can be seen, an unresolvable conflict arises between $D1$ and $D2$. Fig. 32(a) and (b) shows the NAHPF-based PRFs for $D1$ and $D2$. Fig. 33 shows the corresponding locations of the robots at different instants in time. As

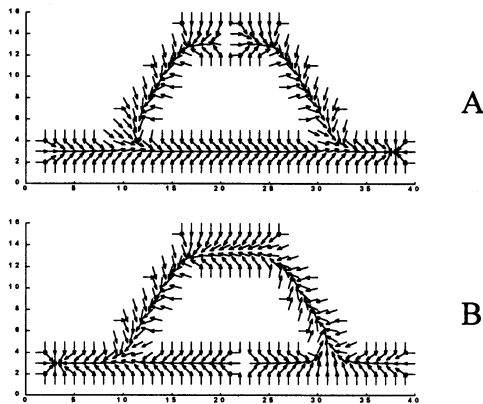


Fig. 32. Gradient field from an NAHPF-based HPC. (a) PRF-1. (b) PRF-2.

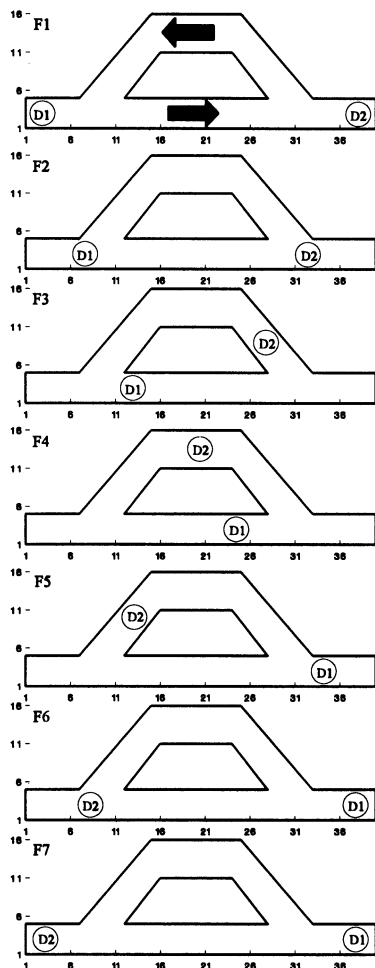


Fig. 33. Success of an NAHPF-based multiagent planner in driving the agents to their respective targets.

can be seen, conflict was resolved by marking the tight passages as one-way streets.

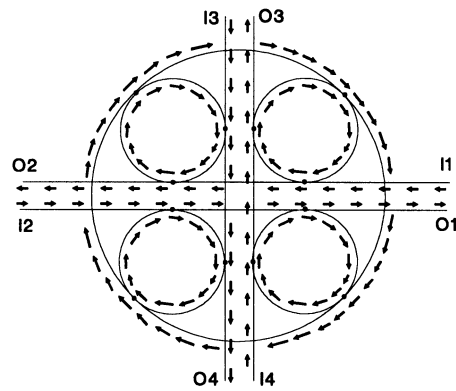


Fig. 34. Highway switch.

E. Highway Switching

One possible application of the NAHPF-based control is highway switching. The aim is to minimize disruption to traffic by sparing a vehicle from having to slow down too much or stop when changing roads, or reversing direction. Coping with this situation requires the design of a highway switching node [5]. This switch may be looked at as a multi-input, multi-output network [93] with the proper topology and geometry. A dynamical system is then induced on this network in order to build a switch that would autonomously control the trajectory of the vehicle concerned in the desired manner. The NAHPF-based control is essential for inducing this type of control on the network. This is illustrated by the following example.

Fig. 34 shows two perpendicular highways intersecting each other. Each highway contains two unidirectional lanes. A switch is placed at the intersection. A lane leading to the switch is marked as an input (I) and a lane leading out of it is marked as an output (O). The circuit used in building the switch consists of four roundabouts symmetrically placed to connect the adjacent lanes of the highway. A large roundabout is also added to link the four smaller roundabouts. The direction of traffic in all roundabouts is constrained to move clockwise. Fig. 35 shows the different routes (solid lines) generated by the switch (dotted lines). As can be seen, no sharp turns appear in the generated trajectories.

VIII. DISCUSSION AND CONCLUSIONS

The method reported in this paper is a part of ongoing work to build a new class of intelligent motion controllers that have a good chance of meeting the demands a realistic environment may present an agent with. The behavior of agents equipped with such controllers is goal-oriented, context-sensitive (i.e., meaningfully react to the events happening in their external environment), and intelligent. This intelligence is measured by an agent's ability to accommodate internal and external factors in generating its actions. It is also related to its ability to act online based on the fragments of data its sensors feedback, as well as its ability to convert this discrete-in-time data flow into a successful continuous-in-time flow of action instructions. The authors strongly believe in the ability of EHPCs to function in this manner.

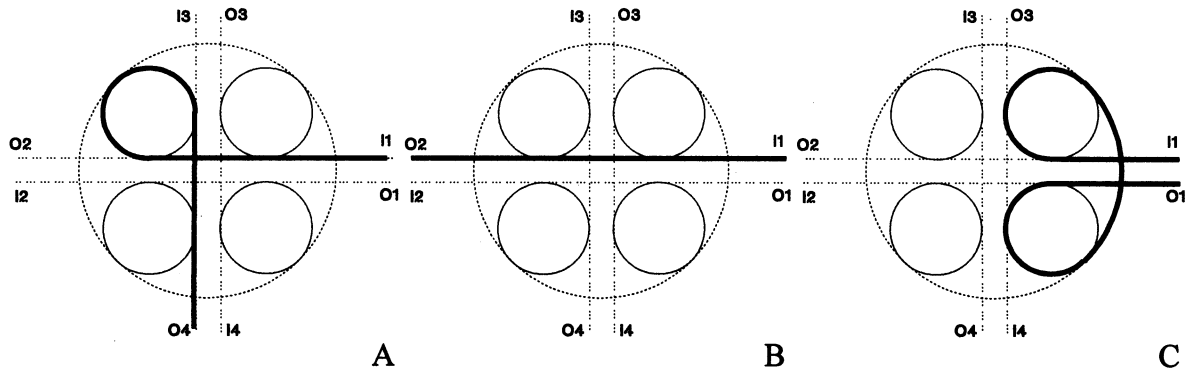


Fig. 35. Paths generated by an NAHPF-based HPC for a vehicle crossing the highway switch. (a) $I1 \rightarrow O4$. (b) $I1 \rightarrow O2$. (c) $I1 \rightarrow O1$.

It is obvious from the above that EHPCs have to be implemented in a declarative mode where no *a priori* known structure is imposed on the control field. Rather, the structure of the controller evolves with the online sensory data feedback taking into account the aim of the control and the constraints on behavior. To obtain the needed lucidity of structure, the control has to be induced by operating on a potential surface with a partial differential operator. The potential field approach, of which the NAHPF is a new addition, is very suitable for use in constructing declarative controllers, especially when configured in a PDE-ODE mode.

An important issue on which the work in this paper assists in shedding some light is the use of evolution versus the use of search (it ought to be noticed that function minimization is a form of search) as a paradigm for action selection. One may conclude that evolution has a more generic nature than search. It allows the handling of a wider class of constraints compared to a search-based method. For example, directional constraints, which are encoded with the aid of relations (not functions), cannot be handled by a search-based approach. Another advantage of evolutionary techniques is their ability to manage the complexity of massive systems such as the interactive collective of microcontrollers composing the AL machine used for converting the database of the agent into a control action.

It is unfortunate that the perception reflected by the sizable literature on HPF's has remained trapped in the classical linear representation of the approach which is stated using Lapalce's equation. NAHPFs are a proof that more rich representations of the HPF approach *do exist*. This brings with it the strong possibility of expanding the horizon of existing motion planners to tackle new and challenging problems in the area.

One last point the authors want to emphasize is the distinct nature of nonholonomic control and NAHPF-based control. Let us first consider the static, nonholonomic system in (47), where

$$\dot{X} = g(u). \tag{47}$$

Any action solicited by u has to filter through g in order to induce a change in X . It is not hard to see that the state is prevented from proceeding along the directions lying in the null space of $g(Ng)$. Unfortunately, such directions are not native to state space. This is illustrated with the help of Fig. 36(a). At a

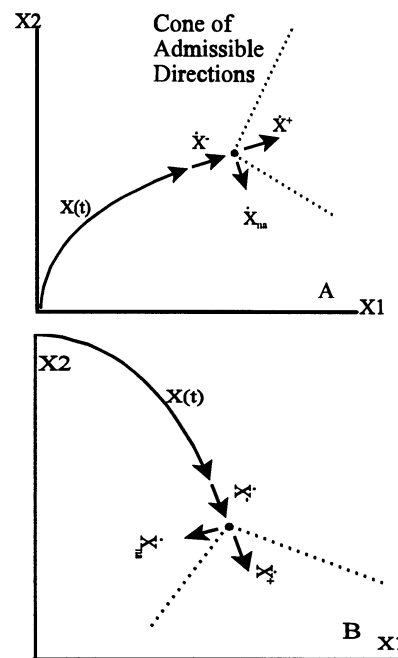


Fig. 36. Floating nature of nonholonomic constraints.

point X_p in state space the inadmissible directions ($\dot{X}_{na} = Ng$) are a function of the previous value of \dot{X} (\dot{X}^-), Fig. 36(a) and (b). Depending of the value of \dot{X}^- , Ng acquires an orientation with respect to the state space coordinates. An admissible direction at X_p (\dot{X}^+) may become inadmissible if the value of \dot{X}^- changes. Therefore, for a nonholonomic controller it is impossible to specify a direction relative to state space coordinates along which the direction of motion may be constrained. As was clearly demonstrated in this paper, this is not the case for NAHPF-based controllers.

The authors are optimistic that further exploration of the HPF approach will reveal many interesting features that could furnish a good basis for tackling difficult problems such as planning with aging information, multiagent multitarget planning in cluttered environments and jointly accounting for the dynamic and kinematic of an agent when planning relying on sensory data feedback only.

REFERENCES

- [1] J. Latombe, *Robot Motion Planning*. Boston, MA: Kluwer, 1991.
- [2] J. Schwartz and M. Sharir, "A survey of motion planning and related geometric algorithms," *Artif. Intell. J.*, vol. 37, pp. 157–169, 1988.
- [3] Y. Hwang and N. Ahuja, "Gross motion planning," *ACM Comput. Surveys*, vol. 24, no. 3, pp. 291–91, Sept. 1992.
- [4] *Manual on Traffic Control Devices, Volume 1: Road Signs and Road Markings*, The Hashemite Kingdom of Jordan, Ministry of Public Work, Traffic and Maintenance Directorate, Amman, Jordan.
- [5] R. Roess, W. McShane, and E. Prassas, *Traffic Engineering*. Englewood Cliffs, NJ: Prentice-Hall, 1998.
- [6] R. J. Wilson, *Introduction to Graph Theory*, Third ed. London, U.K., 1985.
- [7] B. Bollobas, *Graph Theory, an Introductory Course*. New York: Springer-Verlag, 1979.
- [8] H. M. Wagner, *Principles of Operations Research With Applications to Managerial Decisions*. Englewood Cliffs, NJ: Prentice-Hall, 1969.
- [9] H. Kolmanovsky and N. McClamroch, "Developments in nonholonomic control problems," *IEEE Contr. Syst.*, vol. 15, no. 6, pp. 20–36, Dec. 1995.
- [10] C. Hull, "The goal gradient hypothesis and maze learning," *Psychol. Rev.*, vol. 39, no. 1, pp. 25–43, Jan. 1932.
- [11] —, "The goal-gradient hypothesis applied to some 'Field-Force' problems in the behavior of young children," *Psychol. Rev.*, vol. 45, no. 4, pp. 271–299, July 1938.
- [12] L. Loef, "An algorithm for computer guidance of a manipulator in between obstacles," M.S. thesis, Oklahoma St. Univ., Stillwater, OK, 1973.
- [13] L. Loef and A. Soni, "An algorithm for computer guidance of a manipulator in between obstacles," *Trans. ASME, J. Eng. Industry*, pp. 836–842, Aug. 1975.
- [14] O. Khatib, "Real-time obstacle avoidance for manipulators and mobile robots," in *Proc. IEEE Int. Conf. Robotics Automat.*, St. Louis, MO, Mar. 25–28, pp. 500–505.
- [15] B. Krogh, "A generalized potential field approach to obstacle avoidance control," in *Robotics Research: The Next Five Years and Beyond*. Bethlehem, PA, 1984, pp. 1–15.
- [16] —, "Guaranteed steering control," in *Proc. Amer. Contr. Conf.*, Boston, MA, June 19–21, 1985, pp. 950–955.
- [17] M. Takegaki and S. Arimoto, "A new feedback method for dynamic control of manipulators," *Trans. ASME, J. Dyn. Syst., Meas., Contr.*, vol. 102, pp. 119–125, June 1981.
- [18] T. Nishida, A. Yamada, and S. Doshita, "Figuring out most plausible interpretation from spatial constraints," in *Proc. Workshop Spatial Reasoning Multi-Sensor Fusion*, A. Kak and S. Chen, Eds., 1987, pp. 158–167.
- [19] V. Pavlov and A. N. Voronin, "The method of potential functions for coding constraints of the external space in an intelligent mobile robot," *Sov. Automat. Contr.*, vol. 17, no. 6, pp. 45–51, 1984.
- [20] A. Vereshchagin and L. Minayev, "Principles of construction of specialized computers for positional supervisor control of a manipulator," *Eng. Cybern.*, vol. 16, pp. 45–52, July–Aug. 1978.
- [21] V. Malyshev, "A method of constructing program motions of a manipulator," *Eng. Cybern.*, vol. 18, pp. 41–45, Nov.–Dec. 1980.
- [22] G. Aksenov, D. Voronetskaya, and V. Fomin, "A construction of program movements of a manipulator with the aid of a computer," *Eng. Cybern.*, vol. 16, pp. 40–45, July–Aug. 1978.
- [23] A. A. Petrov and I. M. Sirotka, "Control of a robot-manipulator with obstacle avoidance under little information about the environment," in *Proc. 8th IFAC Congr.*, vol. 14, Kyoto, Japan, Aug. 1981, pp. 54–59.
- [24] A. Petrov and I. Sirotka, "Obstacle avoidance by a robot manipulator under limited information about the environment," *Automat. Remote Contr.*, pt. 1, vol. 44, no. 4, pp. 431–440, Apr. 1983.
- [25] J. Andrews and N. Hogan, "Impedance control as a framework for implementing obstacle avoidance in manipulators," in *Contr. Manuf. Process. Robotics Syst.*, D. Hardt and W. Book, Eds., Boston, MA, Nov. 13–18, 1983, pp. 243–251.
- [26] P. Doyle and J. Snell, "Random walks and electric networks," in *The Carus Mathematical Monographs: Number Twenty-Two*. New York: Math. Assoc. Amer., 1984.
- [27] R. Hersh and R. Griego, "Brownian motion and potential theory," *Sci. Amer.*, vol. 220, pp. 66–74, Mar. 1969.
- [28] C. Nash-Williams, "Random walk and electric currents in networks," *Proc. Cambridge Philosophical Soc. (Math. Phys. Sci.)*, vol. 55, pp. 181–194, 1959.
- [29] K. Sato, "Collision avoidance in multi-dimensional space using laplace potential," in *Proc. 15th Conf. Robotics Soc. Jpn.*, 1987, pp. 155–156.
- [30] —, "Deadlock-free motion planning using the laplace potential field," *Adv. Robotics*, vol. 7, no. 5, pp. 449–461, 1993.
- [31] C. Connolly, R. Weiss, and J. Burns, "Path planning using laplace equation," in *Proc. IEEE Int. Conf. Robotics Automat.*, Cincinnati, OH, May 13–18, 1990, pp. 2102–2106.
- [32] E. Prassler, "Electrical networks and a connectionist approach to path-finding," in *Connectionism in Perspective*, R. Pfeifer, Z. Schreier, F. Fogelman, and L. Steels, Eds. Amsterdam, The Netherlands: Elsevier, North-Holland, 1989, pp. 421–428.
- [33] I. Tarassenko and A. Blake, "Analogue computation of collision-free paths," in *Proc. IEEE Int. Conf. Robotics Automat.*, Sacramento, CA, Apr. 1991, pp. 540–545.
- [34] G. Lei, "A neuron model with fluid properties for solving labyrinthian puzzle," *Biolog. Cybern.*, vol. 64, pp. 61–67, 1990.
- [35] E. Plumer, "Cascading a systolic array and a feedforward neural network for navigation and obstacle avoidance using potential fields, NASA Contractor Rep. 177 575," Moffett Field, CA, Ames Res. Cent. Contract NGT-50 642, 1991.
- [36] D. Keymeulen and J. Decuyper, "A reactive robot navigation system based on a fluid dynamics metaphor," *Artif. Intell. Lab., Vrije Univ. Brussel, Brussels, Belgium, AI MEMO # 90-5*, 1990.
- [37] J. Decuyper and D. Keymeulen, "A reactive robot navigation system based on a fluid dynamics metaphor," in *Proc. Parallel Problem Solving From Nature, First Workshop*, H. Schwefel and R. Hartmanis, Eds., Dortmund, Germany, Oct. 1–3, 1990, pp. 356–362.
- [38] S. Akishita, S. Kawamura, and K. Hayashi, "New navigation function utilizing hydrodynamic potential for mobile robot," in *Proc. IEEE Int. Workshop Intell. Motion Contr.*, Istanbul, Turkey, Aug. 20–22, 1990, pp. 413–417.
- [39] G. Cheng and M. Tanaka, "A parallel iterative routing algorithm based on local current comparison method," in *Proc. Int. Conf. Circuits Syst.*, vol. 2, Shenzhen, China, June 16–17, 1991, pp. 651–654.
- [40] G. Cheng, M. Ikegami, and M. Tanaka, "A resistive mesh analysis method for parallel path searching," in *Proc. 34th Midwest Symp. Circuits Syst.*, vol. 2, Monterey, CA, May 14–17, pp. 827–830.
- [41] M. Kanaya, G. Cheng, K. Watanabe, and M. Tanaka, "Shortest path searching for the robot walking using an analog resistive network," in *Proc. ISCAS IEEE Int. Symp. Circuits Syst.*, vol. 6, London, U.K., May–June 1994, pp. 311–314.
- [42] N. Dunskeya and Y. Pyatnitskiy, "The objective potential method in problems of synthesizing controls for manipulator robots," *Sov. J. Comput. Syst. Sci.*, vol. 27, no. 3, May–June 1989.
- [43] Z. Li and T. Bui, "Robot path planning and navigation using fluid model," in *Proc. Second Int. Conf. Automat., Robotics, Comput. Vision*, Sept. 16–18, 1992, pp. RO-10.3.1–RO-10.3.5.
- [44] D. Megherbi and W. Wolovich, "Real-Time velocity feedback obstacle avoidance via complex variables and conformal mapping," in *Proc. IEEE Int. Conf. Robotics Automat.*, Nice, France, May 1992, pp. 206–213.
- [45] J. Kim and P. Khosla, "Real-time obstacle avoidance using harmonic potential functions," in *Proc. IEEE Int. Conf. Robotics Automat.*, vol. 8, June 1992, pp. 338–349.
- [46] S. Akishita, S. Kawamura, and T. Hisanobu, "Velocity potential approach to path planning for avoiding moving obstacles," *Adv. Robotics*, vol. 7, no. 5, pp. 463–478, 1993.
- [47] C. Connolly and R. Grupen, "The application of harmonic functions to robotics," *J. Robotics Syst.*, vol. 10, no. 7, pp. 931–946, 1993.
- [48] J. Guldner and V. Utkin, "Sliding mode control for an obstacle avoidance strategy basen on a harmonic potential field," in *Proc. 32nd Conf. Decision Contr.*, San Antonio, TX, Dec. 15–17, 1993, pp. 24–429.
- [49] D. Keymeulen and J. Decuyper, "The fluid dynamics applied to mobile robot motion: The stream field method," in *Proc. IEEE Int. Conf. Robotics Automat.*, San Diego, CA, May 8–13, pp. 378–85.
- [50] A. Masoud and S. Masoud, "Robot navigation using a pressure generated mechanical stress field 'The biharmonic potential approach,'" in *Proc. IEEE Int. Conf. Robotics Automat.*, San Diego, CA, May 8–13, 1994, pp. 124–129.
- [51] M. Stan, W. Bursleson, C. Connolly, and R. Grupen, "Analog VLSI for path planning," *J. VLSI Signal Process.*, vol. 8, pp. 61–73, 1994.
- [52] J. Guldner and V. Utkin, "Sliding mode control for gradient tracking and navigation using artificial potential fields," *IEEE Trans. Robotics Automat.*, vol. 11, pp. 247–254, Apr. 1995.
- [53] K. Althofer, D. Fraser, and G. Bugmann, "Rapid path planning for robotic manipulators using an emulated resistive grid," *Electron. Lett.*, vol. 31, no. 22, pp. 1960–61, Oct. 1995.
- [54] H. Jacob, S. Feder, and J. Slotine, "Real-time path planning using harmonic potentials in dynamic environment," in *Proc. IEEE Int. Conf. Robotics Automat.*, Albuquerque, NM, Apr. 1997, pp. 874–881.

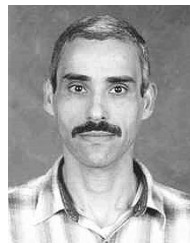
- [55] C. Connolly, "Harmonic functions and collision probabilities," *The Int. J. Robotics Res.*, vol. 16, no. 4, pp. 497–507, Aug. 1997.
- [56] T. Tsuji, P. Morasso, and M. Kaneko, "Trajectory generation for manipulators based on artificial potential field approach with adjustable temporal behavior," in *Proc. IEEE/RSJ Int. Conf. Intell. Robots Syst.*, vol. 2, pp. 438–443.
- [57] I. Mantegh, M. Jenkin, and A. Goldenberg, "A probability-based approach to model-based path planning," in *Proc. IEEE/RSJ Int. Conf. Intell. Robots Syst.*, vol. 2, Grenoble, France, Sept. 7–11, 1997, pp. 1189–1195.
- [58] —, "Solving the find path problem: A complete and less complex approach using the BIE methodology," in *Proc. IEEE Int. Symp. Comput. Intell. Robotics Automat.*, 1997, pp. 115–121.
- [59] —, "A modular and less complex environment representation algorithm," in *IEEE Int. Symp. Industrial Electron.*, vol. 2, Pretoria, South Africa, July 7–10, 1998, pp. 668–673.
- [60] T. Herbert and K. Valavanis, "Navigation of an autonomous vehicle using an electrostatic potential," in *Proc. IEEE Int. Conf. Contr. Applicat.*, Trieste, Italy, Sept. 1–4, 1998, pp. 1328–1332.
- [61] T. Herbert, N. Tsourveloudis, and K. Valavanis, "Fuzzy control of autonomous vehicle navigation utilizing an electrostatic potential field," in *Proc. IEEE Int. Conf. Contr. Applications*, Trieste, Italy, Sept. 1–4, 1998, pp. 658–662.
- [62] S. Sasaki, "A practical computational technique for mobile robot navigation," in *Proc. IEEE Int. Conf. Contr. Applicat.*, Trieste, Italy, Sept. 1–4, 1998, pp. 1323–1327.
- [63] Y. Wang and G. Chirikjian, "A new potential field method for robot path planning," in *Proc. IEEE Int. Conf. Robotics Automat.*, San Francisco, CA, Apr. 2000, pp. 977–982.
- [64] E. Silva Jr, P. Engel, M. Trevisan, and M. Idiart, "Exploration method using harmonic functions," *Robotics Autonomous Syst.*, vol. 40, pp. 25–42, 2000.
- [65] M. Trevisan, M. Idiart, and E. Silva Jr, "Storage of multiple navigation maps using neural networks," in *Proc. V Brazilian Conf. Neural Networks*, Rio de Janeiro, Brazil, Apr. 2–5, 2001, pp. 625–629.
- [66] H. Moon and J. Luntz, "Distributed manipulation by superposition of logarithmic-radial potential fields," in *Proc. IEEE Int. Conf. Robotics Automat.*, Washington, DC, May 2002, pp. 1197–1202.
- [67] C. Louste and A. Liegeois, "Near optimal robust path planning for mobile robots: The viscous fluid method with friction," *J. Intell. Robot Syst.*, pp. 99–112, 2000.
- [68] —, "Path planning for nonholonomic vehicles: A potential viscous fluid field method," *Robotica*, vol. 20, pp. 291–298, 2002.
- [69] Z. Li, C. Suen, T. Bui, and Q. Gu, "Harmonic models of shape transformations in digital images and patterns," in *Proc. 10th Int. Conf. Pattern Recognit.*, Atlantic City, NJ, June 16–21, 1990, pp. 1–7.
- [70] A. Masoud, "Evolutionary action maps for navigating a robot in an unknown, multidimensional, stationary environment, Part I: Controller structure," Internal Paper.
- [71] A. Masoud and S. Masoud, "Evolutionary action maps for navigating a robot in an unknown, multidimensional, stationary, environment, Part II: Implementation and results," in *Proc. IEEE Int. Conf. Robotics Automat.*, Albuquerque, NM, Apr. 1997, pp. 2090–2096.
- [72] A. A. Masoud and S. A. Masoud, "A self-organizing, hybrid, PDE-ODE structure for motion control in informationally-deprived situations," in *Proc. 37th IEEE Conf. Decision Contr.*, Tampa, FL, Dec. 16–18, 1998, pp. 2535–40.
- [73] A. Masoud, "Techniques in potential-based path planning," Ph.D. dissertation, Elect. Eng. Dept., Queen's Univ., Kingston, ON, Canada, 1995.
- [74] C. Langton, "Artificial life," in *Artificial Life SFI Studies in the Science of Complexity*, C. Langton, Ed. Reading, MA: Addison-Wesley, 1988, pp. 1–47.
- [75] I. Asimov, "Runaround," in *Patterns of Psychology: Issues and Prospects*, A. C. Kamil and N. R. Simonson, Eds. Boston, MA: Little Brown, 1973, pp. 4–11.
- [76] R. Brooks, "Intelligence without reason," Mass. Inst. Technol. AI Lab., Memo 1293, 1991.
- [77] S. Masoud and A. Masoud, "Constrained motion control using vector potential fields," *IEEE Trans. Syst., Man, Cybern. A*, vol. 30, pp. 251–272, May 2000.
- [78] Z. Chen, "Analogy, systems, and intelligence," *Cybern. Syst.: Int. J.*, vol. 22, pp. 611–616, 1991.
- [79] B. Streetman, *Solid State Electronic Devices*, Second ed. Englewood Cliffs, NJ: Prentice-Hall, 1980.
- [80] H. B. S. Jeffreys, *Method of Mathematical Physics*. Cambridge, U.K.: Cambridge Univ. Press, 1946.
- [81] O. D. Kellogg, *Foundation of Potential Theory*. New York: Dover, 1929.
- [82] F. D. Murnaghan, *Introduction to Applied Mathematics*. New York: Dover, 1948.
- [83] D. Siljak, *Nonlinear Systems, The Parameter Analysis and Design*. New York: Wiley, 1969.
- [84] N. Krasovskii and J. Brenner, *Stability of Motion, Applications of Lyapunov's Second Method to Differential Systems and Equations With Delay*. Stanford, CA: Stanford Univ. Press, 1963.
- [85] D. Koditschek, "Exact robot navigation by means of potential functions: Some topological considerations," in *Proc. IEEE Int. Conf. Robotics Automat.*, Raleigh, N.C, Mar. 1987, pp. 1–6.
- [86] R. Rektorys, *Variational Methods in Mathematics, Science, and Engineering*. New York: D. Reidel, 1977.
- [87] S. Bergman and M. Schiffer, *Kernel Functions and Elliptic Differential Equations in Mathematical Physics*. New York: Academic, 1953.
- [88] J. LaSalle, "Some extensions of Liapunov's second method," *IRE Trans. Circuit Theory*, vol. CT-7, no. 4, pp. 520–527, 1960.
- [89] W. Hayt and J. Kemmerly, *Engineering Circuit Analysis*, 3rd ed. New York: McGraw-Hill, 1978.
- [90] A. Masoud, "A decentralized, evolutionary, hybrid controller for directing traffic along two-way streets," in *Proc. 35th IEEE Conf. Decision Contr.*, Kobe, Japan, 1996, pp. 4419–4424.
- [91] —, "A hybrid, self-organizing controller for multi-agent, motion planning in a stationary environment," in *Proc. CCA/ISIC/CACSD IEEE Int. Symp. Intell. Contr.*, Dearborn, MI, Sept. 15–18, 1996, pp. 13–19.
- [92] —, "Using hybrid vector-harmonic potential fields for multi-robot, multi-target navigation in a stationary environment," in *Proc. IEEE Int. Conf. Robotics Automat.*, Minneapolis, MN, Apr. 22–28, 1996, pp. 3564–3571.
- [93] R. Roher, *Circuit Theory, An Introduction to the State Variable Approach*. New York: McGraw-Hill, 1970.



Samer A. Masoud received the B.Sc. degree in mechanical engineering (aerospace) in 1987 and the M.Sc. degree in mechanical engineering (applied mechanics) in 1990, both from Jordan University of Science and Technology, Irbid, Jordan. In 1995, he received the Ph.D. degree in mechanical engineering (design and stress analysis/dynamics, and vibration) from the University of Cincinnati, Cincinnati, OH.

He is currently an Associate Professor and the head of the Mechanical Engineering Department at the Jordan University of Science and Technology.

His current interests include stress analysis and design, dynamics and vibration, mechanisms, and applied mechanics.



Ahmad A. Masoud received the B.Sc. degree in electrical engineering with a major in power systems and a minor in communication systems from Yarmouk University, Irbid, Jordan, in 1985. He received the M.Sc. (digital signal processing) and Ph.D. (robotics and autonomous systems) degrees, both in electrical engineering, from Queen's University, Kingston, ON, Canada, in 1989 and 1995, respectively.

He worked as a researcher with the Electrical Engineering Department, Jordan University of Science and Technology, Irbid, Jordan, from 1985 to 1987. He was also a part-time Assistant Professor and a Research Fellow with the Electrical Engineering Department, Royal Military College of Canada, Kingston, from 1996 to 1998. During that time, he carried out research in digital signal processing-based demodulator design for high-density, multiuser satellite systems and taught courses in robotics and control systems. He is currently an Assistant Professor at the Electrical Engineering Department, King Fahd University of Petroleum and Minerals, Dhahran, Saudi Arabia. His current interests include navigation and motion planning, robotics, constrained motion control, intelligent control, and DSP applications in machine vision and communication.